1-2012

# Robust Transmission of Images Based on JPEG2000 Using Edge Information

Amjad Nazih Bou Matar

UAEU Faculty of Engineering

جامعة الإمارات العربية المتحدة
United Arab Emirates University

# Robust Transmission of Images Based on JPEG2000 Using Edge Information

By

Amjad Nazih Bou Matar

Thesis Supervisor

Dr. Qurban Ali Memon

January 2012

# Robust Transmission of Images Based on JPEG2000 Using Edge Information

By

Amjad Nazih Bou Matar

Thesis Supervisor

Dr. Qurban Ali Memon

A thesis submitted to the Faculty of Engineering/Department of Electrical Engineering at United Arab Emirates University in partial fulfillment of the requirement for the degree of **Master of Science** in Electrical Engineering

January 2012

# Robust Transmission of Images Based on JPEG2000 Using Edge Information

By

Amjad Nazih Bou Matar

A thesis submitted to the Faculty of Engineering/Department of Electrical Engineering at United Arab Emirates University in partial fulfillment of the requirement for the degree of **Master of Science** in Electrical Engineering

January 2012

Thesis Supervisor

Dr. Qurban Ali Memon

**Thesis Examining Committee:**

**Prof. Mubarak Shah**

University of Central Florida, Agere Chair Professor of Computer Science

**Dr. Hend Alqamzi**

UAE University, Faculty of Engineering, Department of Electrical Engineering

Amjad Nazih Bou Matar

**United Arab Emirates University, Jan 2012**

*Electrical Engineering Department*
*Faculty of Engineering*
*United Arab Emirates University*
*Al-Ain, United Arab Emirates P.O. Box 17555*
*Tel: +971-3-7133585*
*Fax: +971-3-7623156*

**Supervised by**

**Associate Professor Dr. Qurban Ali Memon**

Department of Electrical Engineering, UAE University

**Reviewed by:**

**Prof. Mubarak Shah**
University of Central Florida, Agere Chair Professor of Computer Science

**Dr. Hassan Hejase, Assoc. Prof.,**
UAE University, Faculty of Engineering, Department of Electrical Engineering

**Dr. Hend Alqamzi, Assist. Prof.,**
UAE University, Faculty of Engineering, Department of Electrical Engineering

# Abstract

In multimedia communication and data storage, compression of data is essential to speed up the transmission rate, minimize the use of channel bandwidth, and minimize storage space. JPEG2000 is the new standard for image compression for transmission and storage. The drawback of compression is that compressed data are more vulnerable to channel noise during transmission. Previous techniques for error concealment are classified into three groups depending on the approach employed by the encoder and decoder: Forward Error Concealment, Error Concealment by Post Processing and Interactive Error Concealment. The objective of this thesis is to develop a concealment methodology that has the capability of both error detection and concealment, be compatible with the JPEG2000 standard, and guarantees minimum use of channel bandwidth.

A new methodology is developed to detect corrupted regions/coefficients in the received images using the edge information. The methodology requires transmission of edge information of wavelet coefficients of the original image along with JPEG2000 compressed image. At the receiver, the edge information of received wavelet coefficients is computed and compared with the received edge information of the original image to determine the corrupted coefficients. Three methods of concealment, each including a filter, are investigated to handle the corrupted regions/coefficients.

MATLAB™ functions are developed that simulate channel noise, image transmission using JPEG2000 standard and the proposed methodology. The objective quality measure such as peak-signal-to-noise ratio (PSNR), root-mean-square error (rms) and subjective quality measure are used to evaluate processed images. The simulation results are presented to demonstrate the performance of the proposed methodology. The results are also compared with recent approaches found in the literature. Based on performance of the proposed approach, it is claimed that the proposed approach can be successfully used in wireless and Internet communications.

# Undertaking

I certify that research work titled "*Robust Transmission of Images Based on JPEG2000 Using Edge Information*" is my own work. The work has not been presented elsewhere for assessment. Where material has been used from other sources it has been properly acknowledged / referred.

Signature of Student
Amjad Nazih Bou Matar

January 2012

# Acknowledgement

I would like to thank Allah Almighty for blessing and giving me strength to accomplish this thesis. I also like to take the chance to thank everyone who helped and supported in reaching this stage of the project and in producing this M.Sc. thesis document.

I would like to express my deep sense of gratitude to my supervisor Dr. Qurban Ali Memon for all his guidance, comments and continuous support throughout the development of this thesis. He was available through the period of my research with his deep knowledge, rich experience, high cooperation, positive attitude, boundless energy and motivation.

I would like also to give a special thank to Dr. Mohammed Binjabr for having introduced me to the topic and having steered my attention to the world of digital signals processing.

I wish to thank the reviewers Prof. Mubarak Shah, Dr. Hend Alqamzi and Dr. Hassan Hejase who (in addition to my supervisor) read and commented on the manuscript. Their comments improved the readability and clarity of the thesis.

My unending appreciation goes to my parents and all my family members as a whole for their love, encouragement, and support in all of my endeavors.

***I dedicate this work to all of you.***

**Amjad Bou Matar**

**January 2012**

# List of Publications

1. Amjad Bou Matar, Qurban Memon, “Error Concealment of Noisy JPEG2000 Coded Images using Edge Information”, Submitted to The 8th International Wireless Communications & Mobile Computing Conference, Limassol, CYPRUS, 2012.

2. Amjad Bou Matar, Qurban Memon, “Edge Based Error Concealment in JPEG2000 Coded Images”, under review in International Journal of Computational Vision and Robotics, Inderscience Publishers, UK.

# Table of Contents

# List of Figures

*Number* *Page*

# List of Tables

*Number* *Page*

# Chapter 1
# Introduction

## 1.1 Background

The two common standards to compress and code images before transmission and storage are JPEG and JPEG2000. The JPEG standard is based on the discrete cosine transform (DCT) while JPEG2000 is based on the Wavelet transform. JPEG is the older standard and still widely used. The JPEG2000 is the newer standard. The original standard for digital images (IS 10918-1, popularly referred to as JPEG) was developed long time before that, and because of the major increase in computer technology later, as well as many research, it was decided that it is the need not only for finding a standard that can make the digital image files as small as possible, but it is also the time for having a new standard that can handle many more aspects. So as well as JPEG 2000 is better at compressing images (up to 20 per cent plus), it can allow an image to be retained without any distortion or loss. So if we send the first part of this 'lossless' file to a receiver, we can have a lossy version that appears like present JPEG. But by continuing to transmit the file, the results will start getting better and better until the original image is restored [1]. It extends the old JPEG by providing more flexibility in both the compression of continuous-tone still image and the access to the compressed data [2]. As an example, we can extract a portion of a JPEG-2000 compressed image and use it in retransmission, storage, display and editing. The communication and multimedia industry are shifting toward the JPEG2000 standard for image transmission and storage. However, the JPEG-2000 is still under improvements to reach the point where it could have its significant place in the world of imaging and telecommunications.

## 1.2 Literature Survey

One may ask, as JPEG compression on large images can still provide outstanding images, why do we need a better compression method? The answer for this question can start by having the fast growth in Internet in mind. As an example, one single frame of HDTV needs more than 6 megabytes of uncompressed information, while in one hour show there are 108,000 frames. Then the uncompressed information needed for one hour show is over 650 megabytes of information which is very equivalent to the storage capacity of current CD-ROM. Let us have another example, digital cameras today have more than 12-mega pixels

per sensor, that needs 36 megabytes of data to store a single color frame. Then if there is a need to store 100 images, then the needed storage is going to be over 3.6 gigabytes. Now one can still buy a storage cards with capacity over 32 gigabytes of storage, and then it could be possible to store around 900 images without compression. But what moving these images around the Internet or other devices like phones or printers in an easy and quick way and without a big loss in the quality of the image? As it can be seen, the most important reason for better compression is the need of transmission of the data. In printers and copying machines, it is important to use compression between the computer and the printing or copying device so the transmission rate could be kept down as well as the cost. Till now, most of the Internet connections that people use daily to download images are less than few megabits per second. According to that, if we need to download one frame of a HDTV signal without compression, we are going to need 48 seconds. This amount of time is significantly slow and not suitable for watching the online HDTV movies. The use of wavelets in the JPEG2000 allows obtaining a high compression ratio and keeping the high image quality at the same time. So it is very efficient in making use of the existing and future telecommunication bandwidths. Many types of images like medical images, high-dynamic range still and motion images, three dimensional graphics… etc require up to 16 bits per pixel per color. Having this in mind it can become very obvious that it is very important to have a high compression method without any artifacts effect, not mentioning the high and growing demand of sending these images through communication networks (including equipment like copiers and printers). The important need of the highly compressed as well as artifacts free image is going to make JPEG2000 a capable of living and sustaining algorithm that can replace the current JPEG which is applied and used till today [3-9]. In order to understand JPEG2000 steps, a block diagram of the JPEG2000 standard is shown in Figure 1.1. The brief discussion of each step is provided below.

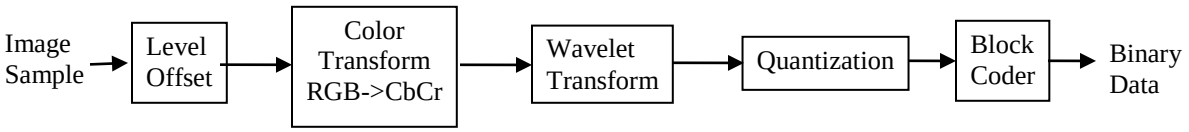


**Figure 1.1:** Block diagram of JPEG2000 Standard

**Level Offset:** It brings an offset to the range of intensity values of the pixels from (0, 255) to (-128, 127). This offset will result in more efficient compression during wavelet transform since pixel intensity will be symmetric around zero.

**Color Transform:** This step transforms a color image to gray level image and two complementary images. These three images are constructed by linear combination of three primary colors red, green, and blue. The three images are considered to be gray level images of intensity that range from -128 to 127 pixel intensity.

**Wavelet Transform:** This transforms the pixel intensity values to wavelet coefficients. This transformation confines the image energy that is distributed uniformly among the pixels into fewer wavelet coefficients. Typically, 93% of the image energy is concentrated into 13% of the wavelet coefficients. The details of this step are discussed below.

**Quantization:** This step divides each coefficient by a specific number and then rounds the result to the nearest integer. This will eliminate typically most wavelet coefficients of higher frequency (higher *sub-band*) since they will be rounded to zeros. This action uses the fact that human visual system is less sensitive to patterns of high spatial frequency.

**Block Code:** This step uses Huffman coding to further compress the image data by converting the decimal values of the coefficients to binary bits. The coefficient values with highest probability of occurrence are coded by fewer bits while coefficients with lower probability of occurrence are coded by more bits.

The discrete version of Wavelet Transform in two dimensions is called two dimensional discrete wavelet transform (2-D DWT). The implementation requires digital filers and down-samplers. With two-dimensional scaling and wavelet functions, the one dimensional fast wavelet transform (1-D FWT) of the rows of $f(x, y)$ is followed by 1-D FWT of the resulting columns. The Figure 1.2 shows the 2-D fast wavelet transform: the input $f(x, y)$ is used as the input $W_\varphi(j+1)$. The rows of the input are convolved with the filters $h_\varphi$ and $h_\psi$ then down sampled by a factor of 2. Both subimages are then convolved again by columns with the filters $h_\varphi$ and $h_\psi$ and down sampled by a factor of 2 to get the four quart-size output sub-images: $W_\varphi(j)$, $W^H_\psi(j)$, $W^V_\psi(j)$ and $W^D_\psi(j)$. In the reconstruction process, the subimages are then unsampled by 2 and convolved with the two one-dimensional filters in two operations one for the subimages' columns and the other is for the subimages' rows. Adding the results is going to yield the $W_\varphi(j+1)$ again which leads to reconstruction of the original image. As an

illustration of image decomposition, the Figure 1.3 shows resulting decomposition of 2-D DWT using three levels of filter banking.

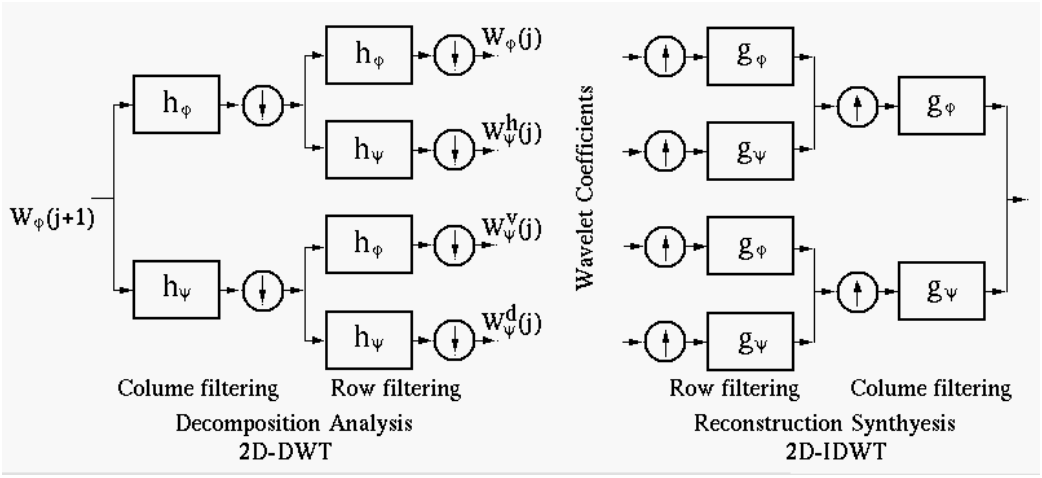


**Figure 1.2:** The analysis filter bank and the synthesis filter bank of the 2-D FWT [10]

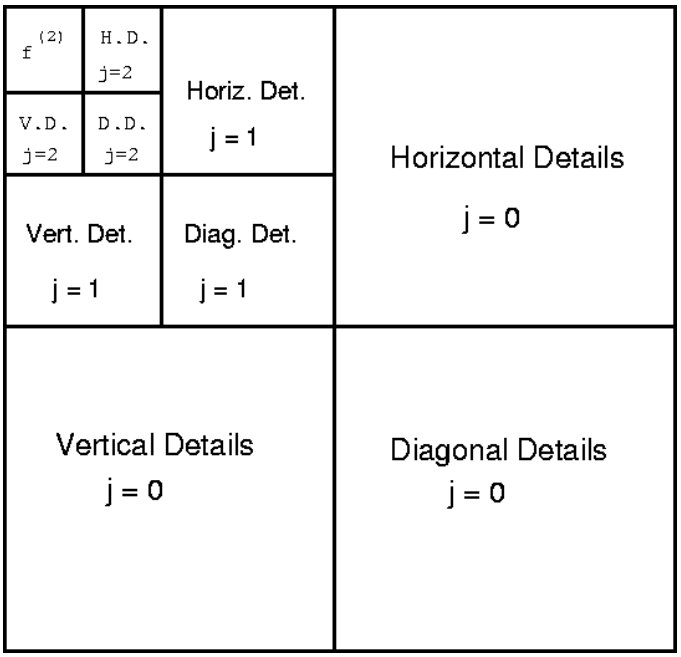


**Figure 1.3:** The resulting decomposition of a 2-D DWT representation of an image [11]

The mathematical operation to obtain wavelet coefficients from the image pixels is given by [12]:

$$W_{\varphi}(j_o,m,n)=\frac{1}{\sqrt{MN}}\sum_{x=0}^{M-1}\sum_{y=0}^{N-1}f(x,y)\varphi_{j_0,m,n}(x,y)$$

$$W_{\psi}^{i}(j,m,n)=\frac{1}{\sqrt{MN}}\sum_{x=0}^{M-1}\sum_{y=0}^{N-1}f(x,y)\psi_{j,m,n}^{i}(x,y)\qquad i=\{H,V,D\} \tag{1}$$

where $\varphi_{j_0,m,n}(x,y)$ is the approximation wavelet function, and $\psi_{j,m,n}^{i}(x,y)$ is the detail wavelet function. The superscript *i* could be *H* for the horizontal detail image, *V* for vertical, and *D* for diagonal. The subscripts *m* and *n* are the location indices of the wavelet coefficient in the detail image, *j* is the level of wavelet decomposition (*sub-band*), and *M* and *N* are the number of rows and columns in the image respectively.

As an illustration, the three levels of Wavelet decomposition will transform an image of size 512 by 512 pixels to a 6-level approximation image of smaller size 64 by 64 and 9 detail (*sub-band*) images of different sizes as shown in Figure 1.4. The nine detail images consist of three 6-level detail images of size 64 by 64, three 7-level detail images of size 128 by 128, and three 8-level detail images of size 256 by 256. The three detail images in each level are called the horizontal $W_{\psi}^{H}(j,m,n)$, the vertical $W_{\psi}^{V}(j,m,n)$, and the diagonal $W_{\psi}^{D}(j,m,n)$ *sub-band*, since they contain information about the horizontal, the vertical, and the diagonal edges of the image respectively. In JPEG2000, typically images are decomposed to seven wavelet levels to accomplish higher compression ratio. The wavelet functions used in JPEG2000 belong to the first member of the Cohen-Daubechies-Feauveauthe family [13]. For reconstruction of the image, the inverse wavelet transform is used at the receiver from the received wavelet coefficients. The inverse wavelet transform is described mathematically as follows [12]:

$$f(x,y)=\frac{1}{\sqrt{MN}}\sum_{m}\sum_{n}W_{\varphi}(j_o,m,n)\varphi_{j_o,m,n}(x,y)+\frac{1}{\sqrt{MN}}\sum_{i=H,V,D}\sum_{j=j_o}^{\infty}\sum_{m}\sum_{n}W_{\psi}^{i}(j,m,n)\psi_{j,m,n}^{i}(x,y) \tag{2}$$

where first term relates to approximation coefficients, and the second term relates to horizontal, vertical and diagonal coefficients.

Image size $M \times N = 512 \times 512$ pixels
If $M = N = 512 = 2^9$
Wavelet Level $J = 9$; $(512 = 2^9)$
$j = j_o, \ldots, J\text{-}1 = 8$

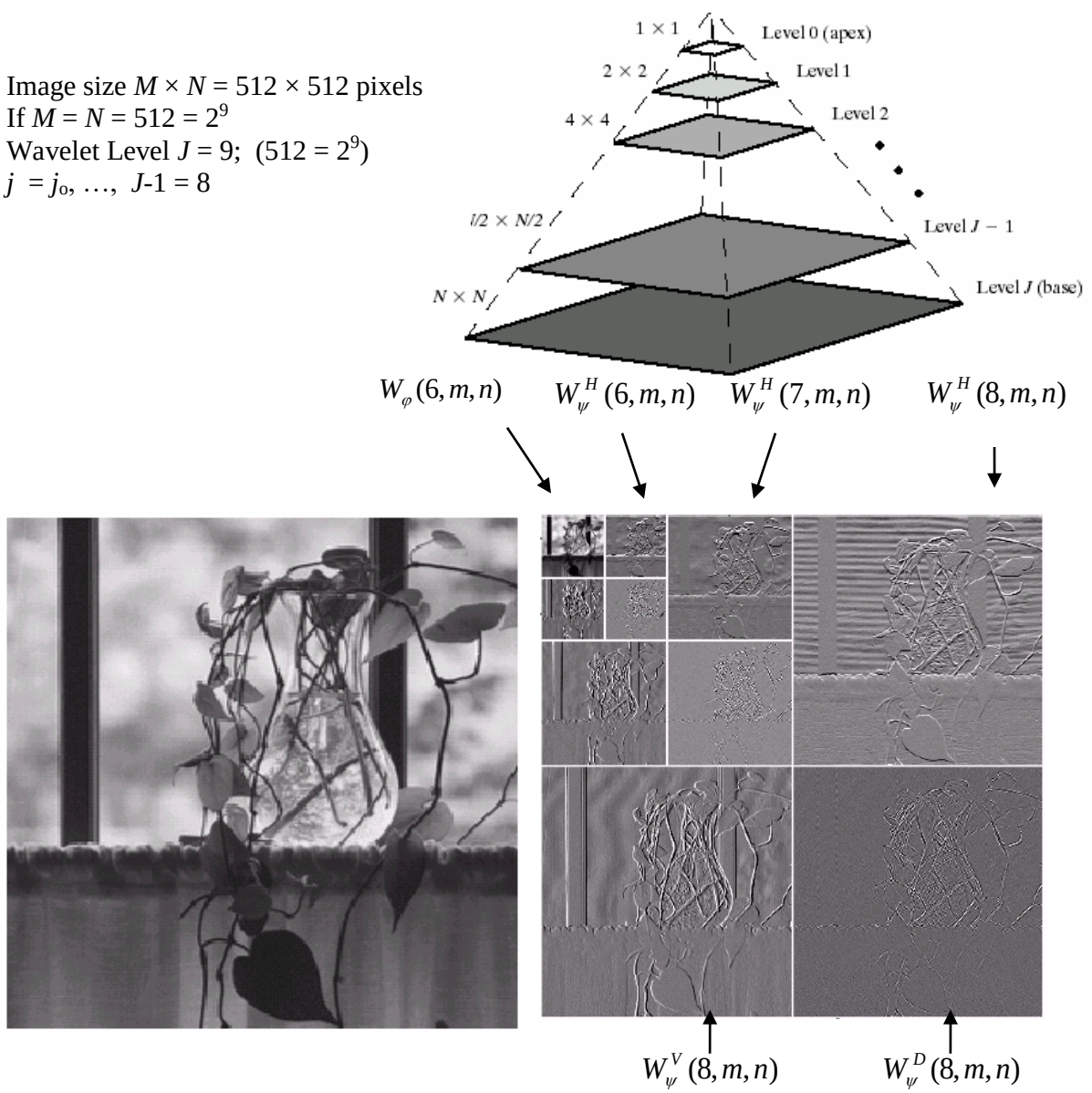


**Figure 1.4:** Original image and the 3-scale-wavelet decomposition [2]

### 1.2.1 Compression and Energy

In order to understand energy in the image, the wavelet transform used here is the two-dimensional discrete wavelet transform (2-D DWT). The energy of an image of size 512 by 512 may be defined as follows:

$$E = \sum_{x=1}^{512}\sum_{y=1}^{512} f(x,y)^2 \qquad (3)$$

where $f(x, y)$ is the pixel intensity value at location $(x, y)$. The energy is usually distributed

uniformly across all pixels of the image. The compression by using wavelet transform is established by confining the image energy into fewer numbers of coefficients so the image can be represented by smaller number of elements. The drawback of image compression is that corruption of small number of wavelet coefficients during transmission results in the corruption of larger area on the received image. For example in Figure 1.4, the wavelet decomposition consists of 3 levels, so a corrupted coefficient in the approximation image will result in the corruption of a block of size 8 by 8 pixels ($2^3 = 8$ pixels). A corrupted coefficient in the detail image at the same level as the approximation coefficient will have the same size of corrupted region but the amplitude of the error is smaller. When the corrupted detail coefficient is at a higher level *sub-band* then the area of corruption as well as the amplitude of the error in the reconstructed image is smaller.

### 1.2.2 Recent Works

In multimedia communications, there are several contradictory system design requirements, for example the minimum use of channel bandwidth while the transmitted data are more resilient to channel noise. Data compression reduces the use of channel bandwidth; however compressed data are more vulnerable to channel noise. Therefore, the transmitted data must be resilient to channel noise [14-17] and other impairments due to channel coding of binary bits [18-20]. Channel coding requires the transmission of more bits.

Several techniques have been proposed in the literature to address the problem of transmission errors by making transmitted data more robust to channel noise and to conceal corrupted data at the receiver. These techniques have been classified into three groups depending on the approach employed by the encoder and decoder. The first technique is Forward Error Concealment at which the encoder plays the major role by making the source data more immune to transmission errors either through source and channel coding such as Reed-Solomon channel coding and multi-description coding (MDC) [21-23]. The second technique is Error Concealment by Post processing in which the decoder plays the major role in concealing errors without depending on additional data from the encoder such as the Spatial Predictive Concealment (SPC) technique [24-26]. The third technique is Interactive Error Concealment (IEC) in which the encoder and decoder work cooperatively through a feedback channel to minimize the impact of transmission errors [27-31]. The aforementioned algorithms require that the corrupted region be identified prior to their error concealment. The algorithm we are proposing has the capability of both error detection and concealment.

The detailed discussion about current and well known correction and concealment techniques is presented later in chapter 3.

### 1.2.3 Current Status of JPEG2000

The Joint Photographic Experts Group (JPEG) is a working group of ISO, the International Organization for Standardization, (ISO/IEC JTC1/SC29/WG1). JPEG is responsible for the popular JPEG Imaging Standard and the JPEG 2000 family of imaging standards. According to the meeting that was held July 18 -22, 2005, in Geneva, Switzerland, hosted by International Telecommunication Union Telecommunication Standardization Sector (ITU-T) and the Swiss National Body, with delegates from 12 countries, the work moved on a variety of technologies within the JPEG 2000 family of standards. These building blocks are going to make the next generation platform for network-enabled imaging. The JP2 file was specified to be the general imaging format of choice.

The Digital Cinema Initiatives (DCI) organization has adopted JPEG 2000 for future distribution of digital movies to theatres. Work has been done between the JPEG committee and the Society of Motion Picture and Television Engineers (SMPTE) for the standardization of the future architecture. The JP3D Ad hoc group is developing the JPEG2000 to three-dimensional images such as CAT scans or scientific simulations (Part 10 of JPEG2000). Continued increase in the interest of JPEG2000 has been noticed from the library and archive community. Part 8 of the JPEG2000 standard (The JPSEC ad hoc group) extended the JPSEC tools and techniques to the JPEG 2000 file format level. JPSEC offered opportunities to make global distribution and e-commerce very secure for digital images.

Wireless applications of JPEG2000 are supported by the JPWL. The JPM standard file format (Part 6 of JPEG2000) is continued in developing to incorporate multiple layered compression formats for document images. Defining a royalty and license fee free entry level JPEG 2000 encoder reached working draft stage. The JPEG committee has always taken on their consideration that open, license-fee free and royalty-fee free standards should be the key to success in the marketplace. That principle was proved with the original JPEG baseline standard. "We are happy with the way JPEG 2000 is getting adopted by various standards groups and organizations", said Dr. Daniel Lee of Yahoo! Inc [1].

JPEG2000 has been solidly stable for several years now. However, its tenuous adoption has raised a question among image software developers regarding the need for continued support. In the fall of 2008, a survey was done regarding the current status of JPEG2000

implementation as a still image format covering heritage institutions involved in digitization. The majority of the survey came from academic research libraries. Among the major issues revealed by repliers, the following surfaced as key ones [32]:

*a.* *Migration Concerns, especially Codec Inconsistency:* Lack of consistency across codecs is an interesting opinion among software vendors.

*b.* *Lack of Adoption due to Misperceived Disadvantages:* A lot of incorrect assumptions are there between JPEG2000's users community. This reveals a real need for better education and understanding:

[1] There is wrong assumption that it is not a true lossless standard.

[2] There is wrong assumption that JPEG2000 cannot support higher bit depth images.

[3] There is unfortunate association of JPEG2000 with JPEG.

[4] There is a wrong impression about JPEG2000 that it is proprietary in nature and not fully documented

## 1.3 Objectives and Thesis Outline

In this thesis, an algorithm is proposed which identifies the corrupted regions in the wavelet domain and executes error concealment in the same domain, without any need to decode the image. The objectives of the thesis are:

a) Develop a method to determine corrupted wavelet regions from the error pattern.
b) Conceal errors in the wavelet domain by setting the values of the corrupted coefficients to zero if these coefficients are located in higher *sub-bands*.
c) Conceal errors in the wavelet domain by estimating the values of the corrupted wavelet coefficients when they are located at the approximation and lower *sub-bands*.

The expected outcomes of this research include:

a) Minimizing the requirement of channel bandwidth and compatibility with JPEG2000 standards
b) Minimizing computational complexity
c) Recommend its use in the wireless and the Internet communications

The rest of the thesis is organized as follows. In the next chapter, a survey of edge detection schemes is presented to highlight strengths and weaknesses of major edge detection schemes. The chapter three discusses well known error detection, correction and concealment techniques that are in use today. In chapter four, proposed approach and its detailed

implementation steps are highlighted, while in chapter five results are presented. The chapter six concludes the thesis work followed by references.

# Chapter 2

# Edge Detection

In this chapter, different edge detection schemes are presented, especially the performance of canny edge detection is highlighted, when there is noise embedded in the image. The relation between edges, low and high frequencies and human visual system is also presented.

## 2.1 Edge Detection

Edge detection is the most useful approach in detecting valuable or important changes in the value of the intensity. This kind of detection is achieved using first order or second order derivative of intensity values. In case of images, the first order derivative is the gradient and in the case of 2-D, function *f(x,y)* is defined as the *vector* of gradients:

$$\nabla \mathbb{f} = \begin{bmatrix} g_x \\ g_y \end{bmatrix} = \begin{bmatrix} \frac{\partial f}{\partial x} \\ \frac{\partial f}{\partial y} \end{bmatrix} \tag{4}$$

This vector has a property that is very important. It points to the direction of the greatest rate of change in *f* at the location *(x,y)*. The *magnitude (length)* of this vector is

$$\nabla f = mag(\nabla \mathbb{f}) = \sqrt{(g_x^2 + g_y^2)} = \sqrt{\left(\frac{\partial f}{\partial x}\right)^2 + \left(\frac{\partial f}{\partial y}\right)^2} \tag{5}$$

This value can be simplified later by either canceling the square root calculation as follows:

$$\nabla f \approx (g_x^2 + g_y^2) \tag{6}$$

or by even just taking the absolute values,

$$\nabla f \approx |g_x| + |g_y| \tag{7}$$

This kind of approximation is still similar to derivative in functionality. It can detect any change in the intensity and have a value related to the degree of change. It is very common to refer to this approximation as the gradient. When there is a change in the intensity, the direction of the gradient vector can be determined by calculating the angle of the maximum rate of change,

$$\alpha(x,y) = \tan^{-1}\left[\frac{g_y}{g_x}\right] \tag{8}$$

The values $g_x$ and $g_y$ are estimated using different edge detectors that are going to be illustrated later in this chapter. The second order derivative for the images is the Laplacian. The Laplacian of a 2-D function *f(x,y)* is:

$$\nabla^2 f(x,y) = \frac{\partial^2 f(x,y)}{\partial x^2} + \frac{\partial^2 f(x,y)}{\partial y^2} \tag{9}$$

It is very rare to use the Laplacian for direct edge detection. The Laplacian is a second derivative, and its sensitivity to noise is very high and unacceptable. The magnitude of the Laplacian produces double edges making it unsuitable for edge detection, and it fails in detecting the direction of the edge. On the other hand, the Laplacian can be very helpful if it is a supplement to other detection methods. As an example, one drawback of the Laplacian (i.e., having double edges) can be used as an advantage with its ability of determining the location of the edge by finding any zero crossing between double edges:

To wrap up here, it can be said that the purpose of the edge detection is to detect location in the image where the intensity has changed in a rapid way by either one or two of the following criteria:

1) Detect a location in the image where the magnitude of the first order derivative of the intensity is greater than a certain threshold.
2) Detect a location in the image where the second order derivative of the intensity has a zero crossing.

Below, brief discussion about well known edge detectors is presented.

### 2.2 Sobel Edge Detector

The Sobel approximation takes the difference between rows and columns in 3 by 3 matrix and is considered as the first order derivative. The middle row and the middle column are multiplied by 2 to avoid the smoothing [33].

$$\nabla f = \sqrt{(g_x^2 + g_y^2)}$$

$$= \sqrt{[(z_7 + 2z_8 + z_9) - (z_1 + 2z_2 + z_3)]^2 + [(z_3 + 2z_6 + z_9) - (z_1 + 2z_4 + z_7)]^2} \tag{10}$$

Where $z_n$ is the intensity element location in a 3 by 3 matrix and *n* varies from 1 to 9. If the gradient $\nabla f(x,y)$ is greater than a certain threshold, then the pixel at the location (x,y) is considered as an edge.

### 2.3 Prewitt Edge Detector

In the Prewitt edge detector, the first order derivative approximation is simply done as the following [33]:

$$\nabla f = \sqrt{(g_x^2 + g_y^2)}$$

$$= \sqrt{[(z_7 + z_8 + z_9) - (z_1 + z_2 + z_3)]^2 + [(z_3 + z_6 + z_9) - (z_1 + z_4 + z_7)]^2} \quad (11)$$

The Prewitt detector is very similar to the Sobel detector but much simpler with somehow more noisy results.

### 2.4 Robert Edge Detector

The equation that approximates the first order derivative here is the diagonal difference [33]:

$$\nabla f = \sqrt{(g_x^2 + g_y^2)} = \sqrt{(z_9 - z_5)^2 + (z_8 - z_6)^2} \quad (12)$$

The Robert Edge Detector is one of the oldest and the simplest edge detectors in the digital image processing. This detector is very limited. It is not symmetric and cannot detect edges that are with angle 45$^o$ or its multiples. These disadvantages are reasons of using this detector less than others, however, it is still found to be useful in some applications where the simplicity and the speed are major factors (e.g, some hardware implementations).

### 2.5 Laplacian of Gaussian (LoG) Detector

With the famous Gaussian function

$$G(x, y) = e^{-\frac{x^2+y^2}{2\sigma^2}}$$

where $\sigma$ is the standard deviation, the Laplacian (second order derivative) is [33]:

$$\nabla^2 G(x, y) = \frac{\partial^2 G(x, y)}{\partial x^2} + \frac{\partial^2 G(x, y)}{\partial y^2}$$

$$= \frac{\partial}{\partial x}\left[\frac{-x}{\sigma^2} e^{-\frac{x^2+y^2}{2\sigma^2}}\right] + \frac{\partial}{\partial y}\left[\frac{-y}{\sigma^2} e^{-\frac{x^2+y^2}{2\sigma^2}}\right]$$

$$= \left[\frac{x^2}{\sigma^4} - \frac{1}{\sigma^2}\right] e^{-\frac{x^2+y^2}{2\sigma^2}} + \left[\frac{y^2}{\sigma^4} - \frac{1}{\sigma^2}\right] e^{-\frac{x^2+y^2}{2\sigma^2}}$$

$$\nabla^2 G(x, y) = \left[\frac{x^2 + y^2 - 2\sigma^2}{\sigma^4}\right] e^{-\frac{x^2+y^2}{2\sigma^2}} \quad (13)$$

The name LoG (Laplacian of Gaussian) detector came from the idea of convolving the image with $\nabla^2 G(x, y)$ which is the same as convolving the image with smoothing function first, then computing the Laplacian of the result. This is because the second derivative is a linear

operation. This convolution blurs the image with a degree of blurring determined by the value of $\sigma$.

### 2.6 Canny Edge Detector

Canny Detection method [34] is the most powerful method. Canny approach was based on three basic objectives:

1) The detector should detect all the edges with no false detection. And at the same time the detected edge should be very close to the correct edge.
2) Edge location should be very accurate. That means the difference between the point marked as an edge and the center of the true edge should be minimized as much as possible.
3) No multi responses for one edge. The detector should give one edge point for each detected edge and should never identify multiple edges in the case of existence of just a single edge.

This approach is done by expressing the three conditions mathematically and then finding the optimal solution for these three mathematical equations. The first step is smoothing the image using a Gaussian filter with a specified standard deviation $\sigma$ to reduce the noise. The second step is to calculate the local gradient $\sqrt{(g_x^2 + g_y^2)}$ and the edge direction $\tan^{-1}\left[\frac{g_y}{g_x}\right]$ for each point. Any of the edge detection methods could be used here and any point that has a maximum local strength in the same direction of the gradient is considered to be an edge point. The third step then is to give a thin line in the output. This is achieved by tracking all the ridges caused by the edge points determined in the second step and set to zero all pixels that are not actually on the ridge top. This process is known as non-maximal suppression. A hysteresis threshold is then used to threshold the ridge pixels. This kind of thresholding uses two thresholds, $T_1$ and $T_2$ where $T_1 < T_2$. Any ridge pixel with a value greater than $T_2$ is considered a strong edge pixel. On the other hand, the ridge pixel that is between $T_2$ and $T_1$ is considered weak. In the final step, the weak pixels are connected to the strong pixels using 8-connectivity which performs edge linking. The Figure 2.1 shows a 600 × 600 image of a building and Figure 2.2 (a-e) show result of the edge detectors: Sobel, Prewitt, Roberts, LoG, Zero crossing and Canny. It is very obvious and noticeable by eye that canny edge detector is the most efficient amongst others.

### 2.7 Edges and Frequencies

As defined before, edge detectors are very useful in detecting the important change in the value of the intensity. That means whenever there is a detection of an edge, at that area there is going to be an important difference between the pixels. This kind of difference denotes the level of variation between intensity densities. Moreover, one of the reasons that could make this variation high is the existence of high frequency (noise) at that area.

**Human visualization and High Frequencies:** Human visual system is less sensitive to high frequency components of the image. Any small change in the low frequency components of the image can be easily noticed by the human eye, but human eye can still appreciate the image even though some manipulation has been done to high frequency components of the image [35]. There are well known filters that operate well on edges while removing noise, like Median filter.

**Median Filter:** The median filter is the best known filter in the category of the nonlinear smoothing spatial filters. It replaces the value of the pixel by median value of the intensity of surrounded pixels including the intensity value of the original pixel itself. Mathematically, it is described as:

$$\hat{f}(x,y) = \text{median}_{(s,t)\in S_{xy}}\{g(s,t)\} \qquad (14)$$

Median filter is widely used because of its capability of reducing certain types of random noises. Media filters have the advantage of making noise reduction with less blurring effect in comparison to linear smoothing filters. These filters are very efficient in case of *impulse noise* that could be also called *salt-and-pepper* noise as it appears as salt or pepper dots distributed along the image. In other words, these filters preserve edges in the image while removing certain kind of noise. The only disadvantage associated with these filters is that these filters are computationally expensive.

**Figure 2.1:** a 600 × 600 image of a building

**Figure 2.2:** (Left to Right, Top to bottom, a-e): The edge detectors for the building image on Figure 2.1: Sobel, Prewitt, Roberts, LoG, Zero crossing and Canny

# Chapter 3

# Error Detection, Correction and Concealment

In this chapter, introduction to different types of errors, their detection and concealment schemes are presented. The objective here is to explore capabilities and weaknesses of different error detection, correction or concealment techniques.

## 3.1 Error and its Types

Error detection in the computer science and telecommunication fields refer to the ability of finding out or discovering errors occurred while transmitting data through noisy and unreliable communication channels. These types of errors may always appear as most of the communication channels are subject to channel noise.

Error detection in general can be achieved by adding extra information to the transmitted data. This kind of information will allow the receiver to find out if there is any defect on the context of the data (i.e., the received message) and can detect certain locations that have been affected by channel noise. Error detection methods can be divided into systematic methods or non-systematic methods [36]. The systematic methods can be simply applied by letting the transmitter to attach a known number of checking bits with the transmitted data. This kind of checking bits can be derived from the original data by any settled algorithm. The receiver can then analyze the received data by applying the same algorithms to them and make a comparison between its output and the received checking bits. When there is a mismatch between the two values, the receiver can consider the point of the mismatching as a point that was affected by an error during the channel transmission. If the system is using a non-systematic method, the transmitter is going to transform the original message and then encode it. This encoded message must have many bits as the original message.

In the case where the capacity of the channel cannot be determined or its variation is very high, the error-detection method can be combined with a system for retransmissions of the incorrect data. This kind of method is called the automatic repeat request method and is highly used in the Internet communications.

Error detection scheme could be selected based on the characteristics of the communication channel. Common channel models include either memory-less models where errors occur randomly and with a certain probability, or dynamic models where errors occur primarily in bursts. Consequently, error-detecting codes can generally be categorized as

random-error-detecting and burst-error-detecting. Some codes can also be suitable for a mixture of random errors and burst errors.

### 3.1.1 Random Errors

When there is an error in the measurement that leads to have a conflict or an inconsistency whenever same measurement is done on the same data, it is termed as a random error. The word random here can indicate totally unpredictable data. It means even if the measurement has been repeated again and again, it is still going to have different numbers every time we repeat it. Random error is caused by the unpredictable fluctuation of the measurement instrument. The concept of the random error is the opposite of the concept of precision. The higher the precision of instrument measuring the data, the smaller the probability of having random results [37-39]. In telecommunication, we can say that the random error happens when there are several errors that are distributed over the received data while these errors can be considered statistically independent from each other.

### 3.1.2 Burst Errors

In telecommunication, a burst error or error burst is a contiguous sequence of symbols, received over a data transmission channel, such that the first and last symbols are in error and there exists no contiguous subsequence of *m* correctly received symbols within the error burst [40]. The integer parameter *m* here refers to the guard band of the error burst. The last symbol in a burst and the first symbol in the following burst are accordingly separated by *m* correct bits or more. The parameter *m* should be specified when describing an error burst. The definition of the length of a burst of bit errors in a frame is the number of bits from the first error to the last one.

## 3.2 Error Detection Schemes

Most commonly, realization of error detection is by using a convenient hash function (or checksum algorithm). It can provide assurance of data integrity by constructing a short “fingerprint of some data. Though if the data is altered, the fingerprint will no longer be valid.

A hash function should be referentially transparent, i.e. if called twice on input that is "equal" (e.g. strings that consist of the same sequence of characters), it should give the same result. This is a contract in many programming languages that allow the user to override equality and hash functions for an object, that if two objects are equal their hash codes must be the same. This is important in order for it to be possible to find an element in a hash table quickly since two of the same element would both hash to the same slot [41].

In some cases, hash functions can be replaced with some other alternative methods such as Random-error-correcting codes based on minimum distance coding which could be very suitable for the cases where a strict guarantee on the minimum number of errors to be detected is desired. Codes described below, are special cases of error detection codes. Although they are rather inefficient, they still can find some applications of error detection because of their simplicity.

### 3.2.1 Repetition Codes

The idea behind the repetition coding scheme is simply repeating every data for a certain amount of time to achieve error-free communication. For each data to be transmitted, these data are divided into certain amount of blocks, while each block is repeated for a suitable number of times. As an example, if we want to send the bit pattern "1011", the four-bit block can be repeated three times, the result will be then "1011 1011 1011". Now, in case error happens and this twelve-bit pattern was received as "1010 1011 1011" – where the first block is not the same as the other two, it is easy to determine that an error has occurred. The advantage of the repetition codes is that they are very simple, however, the efficiency of the repetition code is low in general, in case the error happened in the same place of the three blocks in the previous example "1010 1010 1010" then it would be detected as correct [41].

### 3.2.2 Parity Bits

The idea here is adding a bit to a group of source bits to ensure that the number of set bits in the outcome is even or odd. This scheme is very simple and can be used in detection of any odd number of errors in the output. However, if the flipped bits number is even, it is going to make the parity bit appear correct while the data are incorrect. There are more variations and extensions on the parity bit mechanism such as horizontal redundancy checks, vertical redundancy checks, and "double," "dual," or "diagonal" parity bits.

### 3.2.3 Checksums

The modular arithmetic sum of message code words where the word length is fixed is called the checksum. The means of a ones'-complement may negate this sum prior to transmission in order to detect the resulting errors in all-zero messages. Luhn algorithm and the Verhoeff algorithm [42] are examples of checksum schemes that are designed for specific purposes such as detecting errors commonly introduced by humans in writing down or remembering identification numbers. Checksum schemes include parity bits, check digits, and longitudinal redundancy checks.

### 3.2.4 Cyclic Redundancy Checks (CRCs)

The main use of the cyclic redundancy check (CRC) is to detect accidental changes to digital data in computer networks. CRC is a single-burst-error-detecting cyclic code and non-secure hash function. It is characterized by specification of a so-called generator polynomial. The input data is going to be divided by that polynomial over a finite field, and the remainder becomes the result. One of the favorable properties of Cyclic codes is that they are well suited for detecting burst errors. Moreover, it is easy to implement CRCs in hardware, and according to that they are highly used in digital networks and storage devices such as hard disk drives. Parity can be considered as a special case of a cyclic redundancy check, where the single-bit CRC is generated by the divisor x + 1 [41].

### 3.2.5 Cryptographic Hash Functions

If the changes to data happen accidentally only (i.e., if errors occur in transmission) then the cryptographic hash function can be considered as a strong assurance about data integrity. If any error happen to the data, it is easy to detect that because of the mismatching hash value. Moreover, it is infeasible to find some input data with a given hash value (producing the same hash value). Message authentication codes also called as keyed cryptographic hash functions, can provide additional protection against intentional modification by an attacker [41].

## 3.3 Error-correcting Codes

Error-correcting code can always be used for error detection. Let us consider a code with minimum Hamming distance, $d$. This code can detect up to $d - 1$ errors in a code data. Use of minimum-distance-based error-correcting codes for error detection is very suitable if a strict limit on the minimum number of errors to be detected is desired. If the minimum Hamming distance $d$ in the code is equal to two, this code can be considered as a degenerate case of an error-correcting code, and can be used to detect single errors. The parity bit is an example of a single-error-detecting code [43].

## 3.4 Error Concealment Methods

In multimedia communications, there are several contradictory system design requirements, such as the minimum use of channel bandwidth while the transmitted data are more resilient to channel noise. Data compression reduces the use of channel bandwidth; however compressed data are more vulnerable to channel noise. Therefore, the transmitted data must be resilient to channel noise and other impairments by channel coding the binary

bits [18-20]. The channel coding requires transmission of more bits. Several techniques have been proposed in the literature to address the problem of transmission errors by making the transmitted data more robust to channel noise and to conceal corrupted data at the receiver. These techniques have been classified into three groups depending on the approach employed by the encoder and decoder.

### 3.4.1 Forward Error Concealment

The first technique is Forward Error Concealment at which the encoder plays the major role by making the source data more immune to transmission errors either through source and channel coding such as Reed-Solomon channel coding and multi-description coding (MDC). The main two purposes in the forward error concealment technique are to decrease the effect of errors that could occur in the transmitting channels to minimum in order to cancel the need of error concealment in the decoder; and to make the decoder error concealment more effective. As examples for forward error concealment, we mention the joint source, channel coding and layered coding.

Two types of distortion could be observed at the decoder when using the forward error concealment technique. The first one is the noise that is related to the quantization introduced by the waveform coder. The second one is the transmission errors distortion. The source coder and transport coder here should be designed to minimize the effect of both quantization errors and transmission errors. Forward error concealment can be achieved in many methods. The common thing between these methods is that they all add a controlled amount of redundancy in either the source coder or the transport coder. For the source coder, the redundancy can be added either to waveform coder or to the entropy coder. Moreover, there are some techniques that require cooperation between the source and transport coders, while others may leave some redundancy in or add extra information to the coded data to help error concealment at the decoder. There are also some techniques where the network implements different levels of quality of service control for different sub streams. On the other hand, the assumption could be an equal path [21-23].

### 3.4.2 Error Concealment by Post Processing

The second technique is error concealment by post processing such as the Spatial Predictive Concealment (SPC) technique. In error concealment by post processing technique, the decoder plays the major role in concealing errors without depending on additional data from the encoder. This could be achieved by using different methods such as estimation and

interpolation, spatial and temporal smoothing. In the case of image transmission, some facts can be used in the concealment process of the artifacts caused by transmission errors. As an example, the well-known fact is that the natural scenes images have low frequency components dominating. The values of colors of spatial and temporally adjacent pixels are varying smoothly unless there are regions with sharp edges. Other fact is that the human eyes are able to tolerate more distortion to high frequency components than to the low frequency components. To accomplish error concealment, all the post processing techniques divide the frame into macroblocks. They all make use of the correlation between a damaged macroblock and its adjacent macroblocks in the same frame and/or the previous frame. Some of the techniques only apply to macroblocks coded in intra-mode, while others although applicable to inter-coded blocks, neglect the temporal information [24-26].

### 3.4.3 Interactive Error Concealment (IEC)

The third technique is interactive error concealment (IEC) in which the encoder and decoder work cooperatively through a feedback channel to minimize the impact of transmission errors. Two examples to be quoted here are the ARQ and selective predictive coding based on feedback from the decoder. The idea here is based on the assumption that if a backward channel from the decoder to the encoder is available, better performance can be achieved if the encoder and decoder can cooperate (i.e. either at the source coding or transport level) in the process of error concealment. According to the feedback information from the decoder, the coding parameters at the source coder can be adapted. The percentage of the total bandwidth used for forward error correction or retransmission can be changed based on the employment of the feedback information at the transport level [27-31].

The aforementioned algorithms require that the corrupted region be identified prior to respective error concealment. The algorithm we are proposing in the next chapter has the capability of both error detection and concealment.

# Chapter 4

# Proposed Method and Implementation

In this chapter, an algorithm is proposed for error detection and concealment of corrupted regions in images caused by transmission over a noisy wired or wireless channel. The expected main advantages of the proposed method are the minimum requirement of channel bandwidth and its compatibility with JPEG2000 standard. The proposed method consists of a number of steps to be accomplished: transmission of the image through noisy channel followed by processing of the received signal at the receiver. The proposed algorithm is shown in Figure 4.1. In the following paragraphs, each of its steps is detailed.

## 4.1 Proposed Method

### Step 1: Error detection

In order to understand this step, let us describe what is available at the receiver. At the transmitter, an image is compressed using JPEG2000 standard and transmitted through the channel. Additionally, edge image is also extracted from wavelet coefficients and transmitted through the channel. As the size of the edge image is significantly lower than the compressed, it can be coded using robust channel coding schemes to void distortion due to noise. Thus it is assumed that it is correctly received at the receiver. So at the receiver, noisy compressed image and noise free edge image are received.

At the receiver, received image is channel decoded before edge is extracted. Once edge is extracted from wavelet coefficients image, it is termed as extracted edge image respectively. Next extracted edge image is subtracted from the received edge image of the original image. If the difference between the received edge image and the extracted edge image is zero or below a certain threshold level then the received image is correct or corruption is unobjectionable. In the case where the received edge image differs from the extracted edge image at different regions, these regions are marked as corrupted regions. In JPEG2000, the corrupted regions will have different sizes since the wavelet coefficients at different levels represent different sizes of blocks in the reconstructed image. The block sizes can range from 2 by 2 pixels to 32 by 32 pixels, and generally this depends how many levels of wavelet transform are computed at the transmitter. The spatial pattern of the corrupted region may help to determine if the corrupted region is in the horizontal, vertical, or diagonal *sub-band*.

As an illustration, original image, transmitted edge image, received image mixed with noise, and extracted edge image are shown in Figure 4.2, 4.3, 4.4 and 4.5 respectively. The result of subtracting two edge images is shown in Figure 4.6 to identify corrupted coefficients.

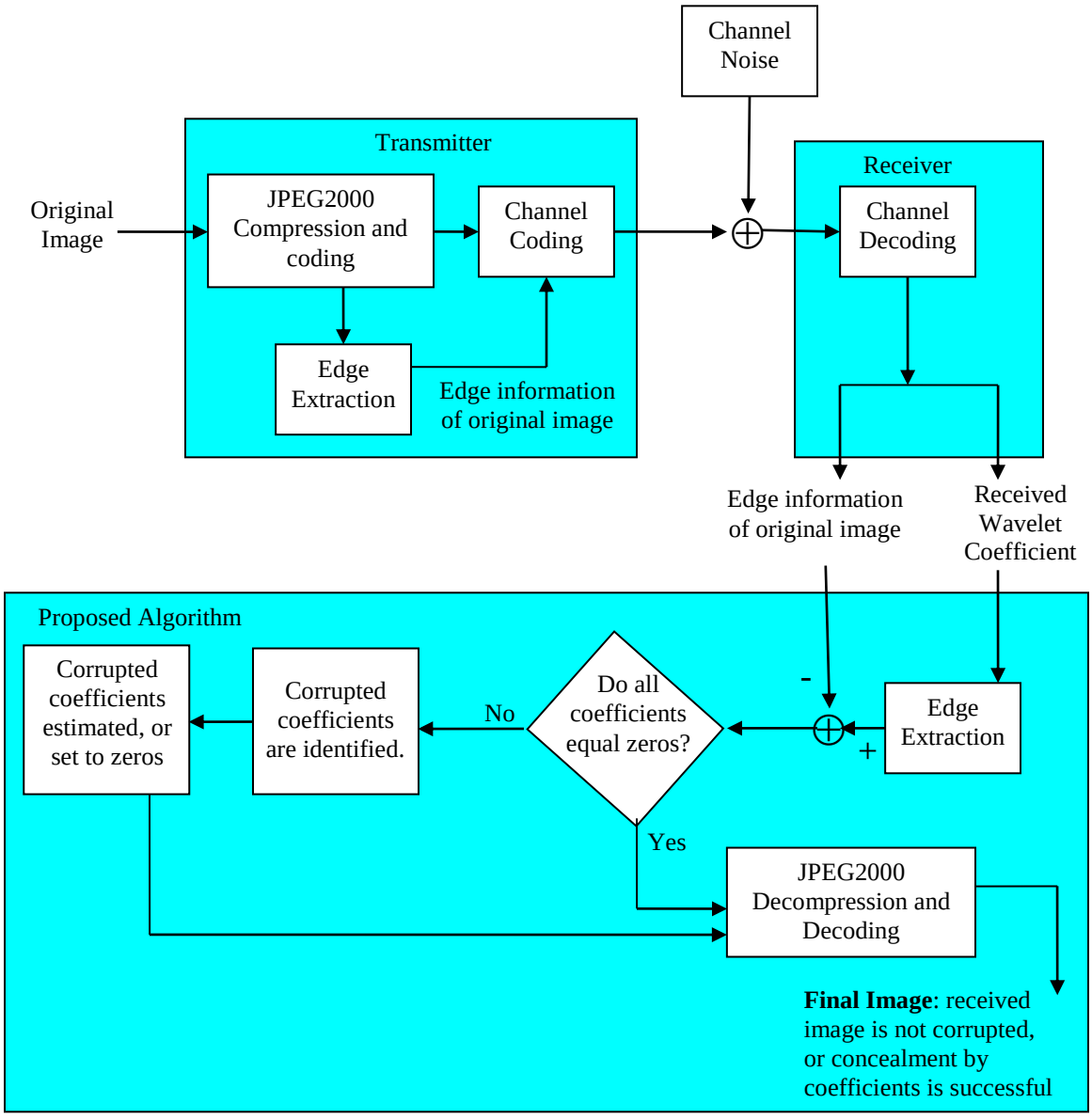


**Figure 4.1:** Block diagram of transmitter, receiver, and proposed algorithm

**Step 2: Concealing errors at higher *sub-band***

This step deals with existence of the corrupted regions or blocks of wavelet coefficients of the received wavelets coefficients. The location of the corrupted block in the received wavelet coefficients may be used to determine the location of the wavelet coefficient within the *sub-band*. Or, all of these sub-bands may be processed in parallel to determine corrupted

wavelet coefficients. Once it is possible to locate the corrupted wavelet coefficients, then their values are set to zero if the coefficients belong to higher sub-bands at lower level or may be estimated by adjacent coefficients if the coefficients belong to higher sub-bands at higher level. Then the image is reconstructed. The loss of image information by setting the values of the wavelet coefficients to zero is unobjectionable especially for coefficients located at higher *sub-bands*.

**Step 3: Concealing errors at lower *sub-band***

If the corrupted coefficients are in the lower *sub-band* then it is proposed to estimate their values from the neighborhood of affected coefficients. For example, if the corrupted coefficients are the approximation coefficients, then it is proposed to estimate their values using the uncorrupted adjacent approximation coefficients.

**Figure 4.2:** Original image

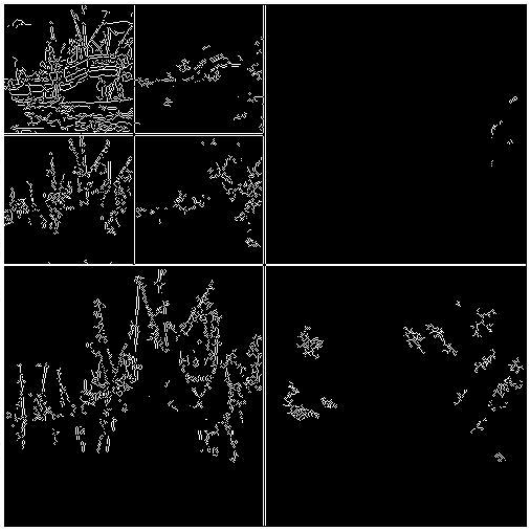

**Figure 4.3:** Transmitted Edge image

**Figure 4.4:** Received image mixed with noise

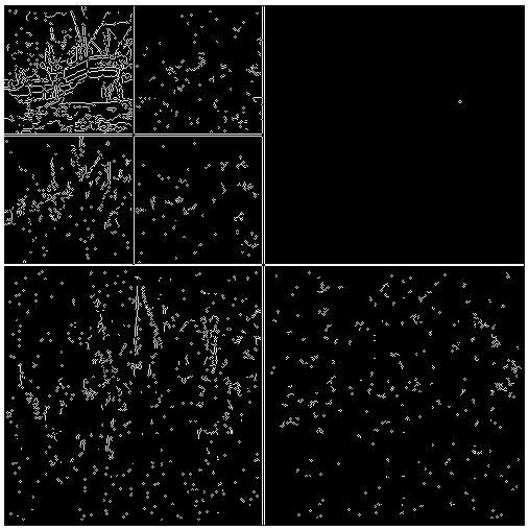

**Figure 4.5:** Extracted edge image

**Step 4: Concealment in the spatial domain (Optional)**

After estimating the values of the corrupted coefficients in the wavelet domain, the image is constructed. There are two possibilities: the first is that the image is completely corrected by estimating the values of the coefficients in the wavelet domain; the second possibility is that some of the corrupted regions are still present, so if desired, the corrupted regions may be further concealed in the spatial domain. This optional step is not shown in Figure 4.1. To conceal the persistent corrupted regions, the edge information of the original image is again used to estimate corrupted pixels. The edge information is expected to classify regions based on intensities. Each corrupted pixel may be estimated by the median intensity of the neighboring uncorrupted pixels located in the same region. By doing so, the original edges and boundaries are preserved. Preserving the edge information of the corrupted image using median filter enhances the subjective quality of the recovered received image.

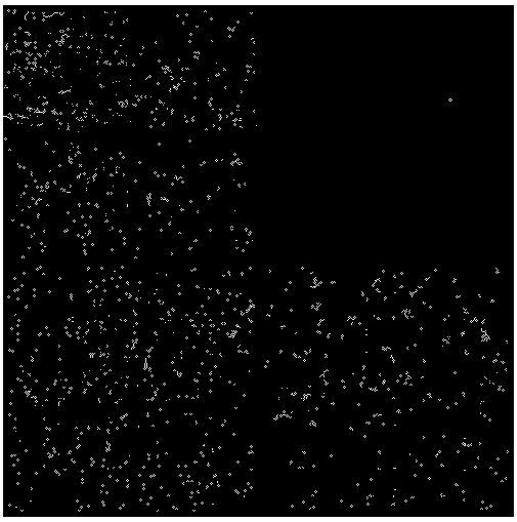

**Figure 4.6**: Locations of corrupted coefficients

### 4.2 Algorithm Implementation Details

Based on the proposed approach, implementation of the algorithm was started to accumulate the results. The following steps are followed:

#### 4.2.1 Wavelet Transform and Its Parameters

After computing the $N_L$ –scale wavelet transform, the total number of transform coefficients is equal to the number of samples in the original image. However, as said before the important visual information is concentrated in fewer coefficients. The quantization operation can then reduce the number of bits needed to represent these coefficients by the following equation [2]:

$$q_b(u,v) = sign[a_b(u,v)] \cdot \text{floor}\left[\frac{|a_b(u,v)|}{\Delta_b}\right] \quad (15)$$

Where $q_b(u,v)$ is the quantized value of the coefficient $a_b(u,v)$ of the sub-band *b*. The "sign" operation represents the famous *Signum* function that returns 1 if the element is greater than zero, 0 if it equals zero and -1 if it is less than zero. The "floor" operation represents the *floor* function, which rounds the elements of any number X to the nearest integers towards minus infinity. The $\Delta_b$ is known as the quantized step size and it is defined as [2]:

$$\Delta_b = 2^{R_b - \varepsilon_b}\left(1 + \frac{\mu_b}{2^{11}}\right) \quad (16)$$

where $R_b$is the nominal dynamic range of sub-band *b*, while $\varepsilon_b$and $\mu_b$are number of bits assigned to the exponent and mantissa of sub-band coefficients. The nominal dynamic range

of sub-band *b* is the sum of the number of bits used to represent the original image and the analysis gain bits for sub-band *b*. The sub-band analysis gain bits follow the simple pattern as shown in Figure 4.7a. Let us take the sub-band b=1 *HH* as an example, there are two analysis gain bits for this sub-band (the number in the small black square).

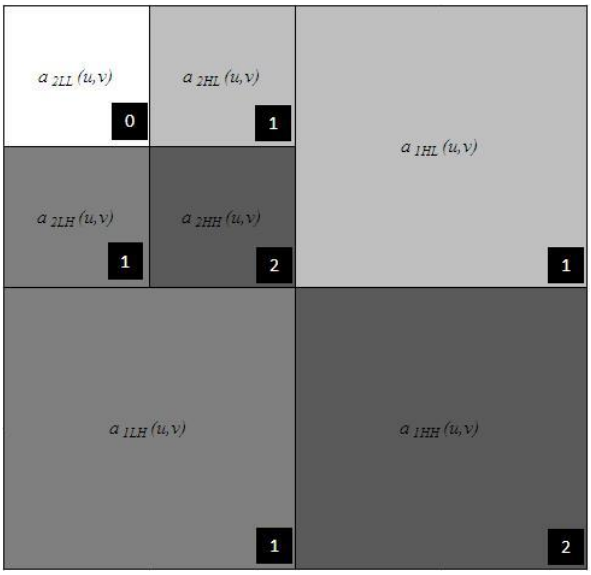


**Fig. 4.7a:** JPEG2000 wavelet transform coefficient notations when $N_L$ = 2. The numbers in the black squares represents that analysis gains

Error-free compression requires the following values, $\mu_b$= 0 and $R_b$= $\varepsilon_b$ so that we can have $\Delta_b$=1. In case where the compression is irreversible, there is no specific quantization step. Instead, the *explicit quantization* or the *implicit quantization* could be implemented. The idea of the explicit quantization is simply having the number of exponent and mantissa bits to be provided to the decoder on a sub-band basis, while in the case of the implicit quantization these numbers of exponent and mantissa are provided for the $N_L LL$ sub-band parameters. By allocating the numbers $\varepsilon_b$and $\mu_b$ to the $N_L LL$ sub-band, the extrapolated parameters for sub-band *b* are

$$\mu_b = \mu_0 \quad (17)$$

$$\varepsilon_b = \varepsilon_0 + nsd_b - nsd_0 \quad (18)$$

Where $nsd_b$ is the number of the sub-band decomposition levels from the original image to the sub-band *b*. At final step of the encoding process, the quantized coefficients are coded arithmetically on a bit-plane basis. The arithmetic coding can be defined as the variable-length coding procedure that is designed to reduce coding redundancy (Huffman coding is an example of this). A MATLAB™ function was developed to resemble the JPEG2000 coding

process, as shown in Figure 1.1. However, the block of coder was not represented by an arithmetic coding, but it has been replaced by Huffman encoding augmented by zero run-length coding for simplicity.

The decoder of JPEG2000 just inverts the previous described operations. The arithmetically coded coefficients are decoded first then a user-selected number of the original image sub-bands are reconstructed. This means that the decoder might have the ability to encode arithmetically $M_b$ bit-planes for a particular sub-band, however user may choose to decode only $N_b$ bit-planes. The step size of $2^{M_b-N_b} \cdot \Delta_b$ is then used to quantizing the coefficients. All the non-decoded bits are set to zero and the resulting coefficients intended as $\bar{q}_b(u,v)$ are denormalized using:

$$R_{q_b}(u,v) = \begin{cases} (\bar{q}_b(u,v) + 2^{M_b-N_b}) \cdot \Delta_b & \bar{q}_b(u,v) > 0 \\ (\bar{q}_b(u,v) - 2^{M_b-N_b}) \cdot \Delta_b & \bar{q}_b(u,v) < 0 \\ 0 & \bar{q}_b(u,v) = 0 \end{cases} \quad (19)$$

where $R_{q_b}(u,v)$ represents the denormalized transform coefficient and $N_b(u,v)$ is the number of decoded bit-planes for $\bar{q}_b(u,v)$. The approximation of the original image is then obtained by calculating the discrete inverse wavelet transform of the denormalized coefficients followed by level shifting the results. As an example, the Figure 4.7b shows the 512 × 512 8-bit monochrome image "Tracy". The JPEG2000 approximation of this image is shown in Fig. 4.8.

**Figure 4.7b:** The 512 × 512 8-bit monochrome image "Tracy"

The Figure 4.8(a) was reconstructed from encoding the original image with a compression ratio of 42:1. While Figure 4.8(b) shows the compression ratio of the encoding set at 88:1. These two results were obtained under the condition of using a five-scale transform and an implicit quantization with $\mu_0$=8 and $\varepsilon_0$= 8.5 and 7, respectively.

Using subjective approach (i.e., a visual comparison between Figure 4.8(a) and Figure 4.8(b)), it is very obvious that when the level of compression increases to 88:1, there is a loss of texture in the woman's clothes and blurring of eyes. These both effects are visible also in Figure 4.4(f). The root mean square (rms) error of the image in Figure 4.8(a) is 3.6 while it is about 5.9 for the image in Figure 4.8(b). The Figures 4.8(c) and Figure 4.8(d) show the difference between the original image and the images on Figure 4.8(a) and Figure 4.8(b) respectively. Using visual comparison, it can be noticed that the difference between the original image and the reconstructed image is higher in Figure 4.8(b), which leads to a higher value in the rms error.

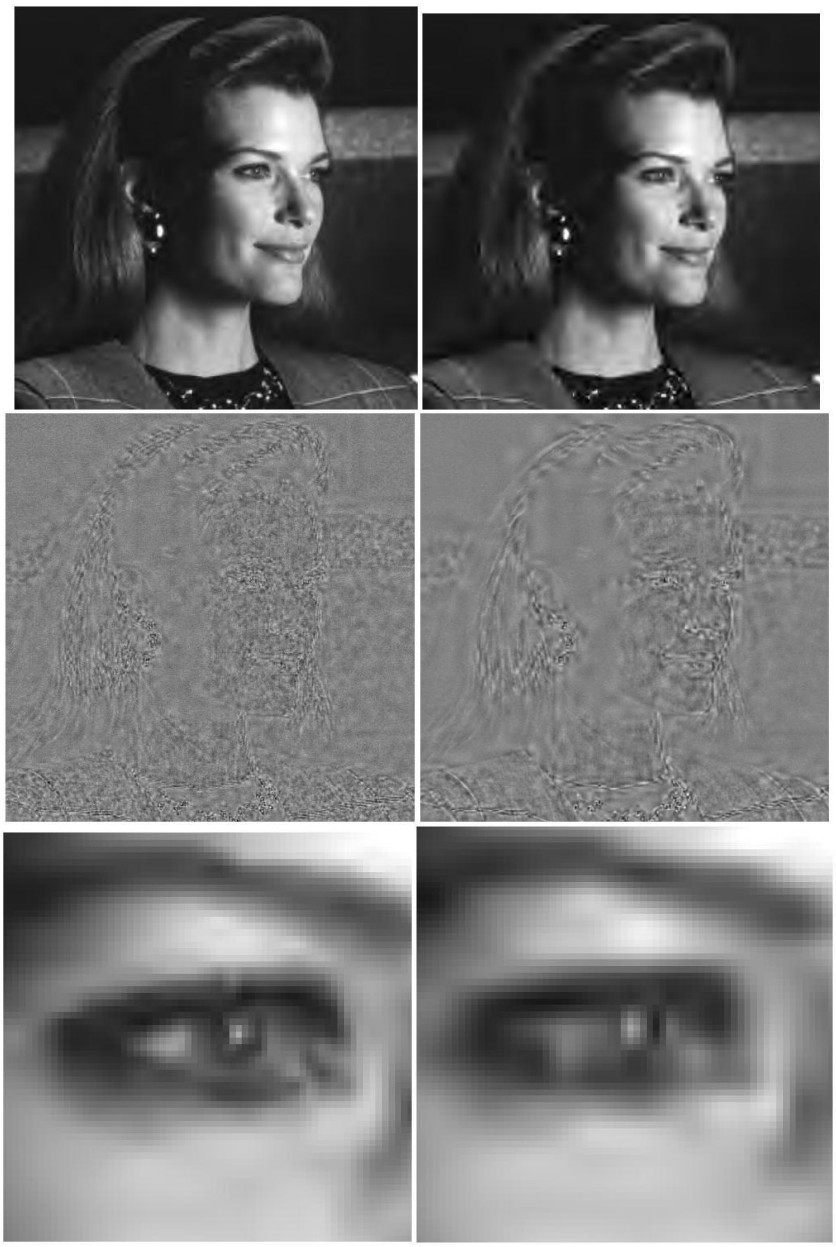

**Figure 4.8:** From right to left, top to bottom: a, b, c, d, e, f. The left column is the JPEG2000 approximation using five scales with implicit quantization with $\mu_0$=8 and $\varepsilon_0$= 8.5. The right column uses $\varepsilon_0$= 7.

### 4.2.2 Edge extraction

Obtaining the wavelet transform is in reality getting the coefficients of the two-dimensional output array from the analysis filter bank, as illustrated on the left side of the Figure 1.2. After going through iterations of the filter bank, the resulting image produces quarter-size coefficient arrays. These coefficients are arranged as a 2 × 2 array of sub-matrices that replace the two-dimensional input from which they are derived. A MATLAB™

code was developed to display these coefficients by performing a similar sub-image composition.

A Canny edge detector is applied to the formulated image with convenient thresholds and then this binary edge information (known as edge image) is sent through the channel. The Figure 4.9(a), 4.9(b), 4.9(c) and 4.9(d) show 512 × 512 8-bit monochrome image “boat”; the wavelet transform of the same image using a five-scale transform with implicit quantization, $\mu_0$=8, $\varepsilon_0$= 8.5; the displayed wavelet coefficients; and edge extraction of the displayed wavelet coefficients respectively.

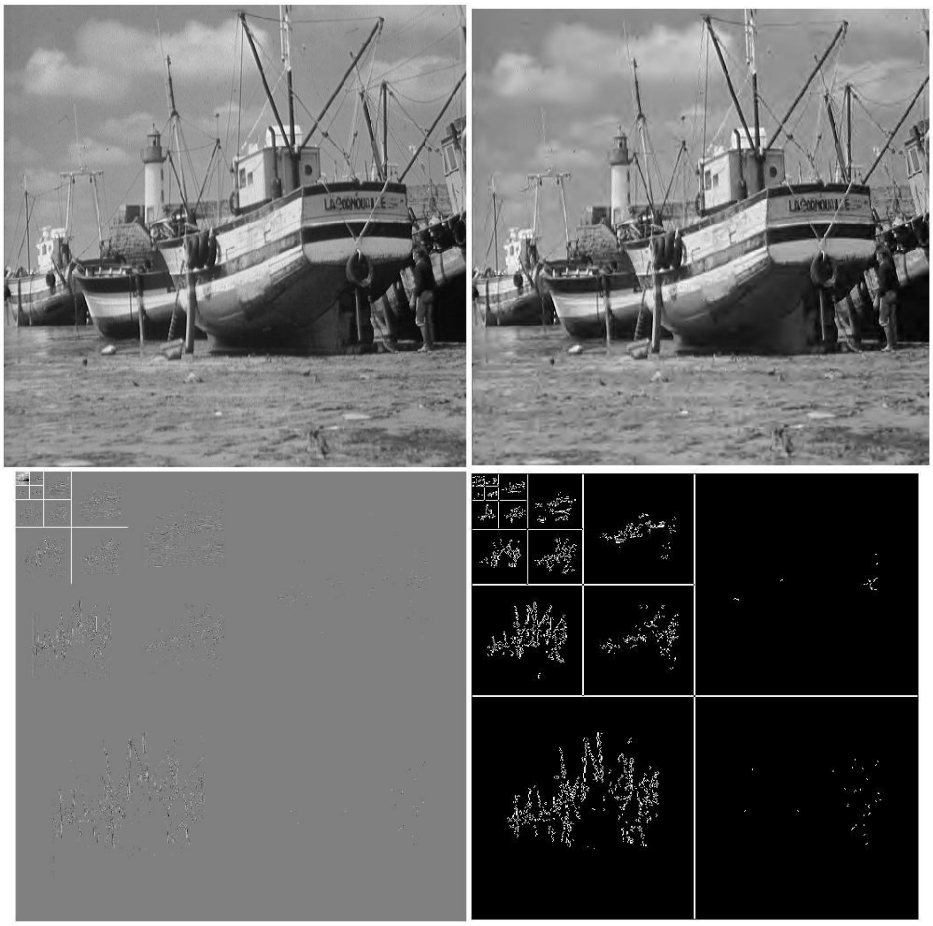

**Figure 4.9:** Top left, bottom left, top right, bottom right (a) Original image (b) The JPEG 2000 approximation using five-scale transform and implicit quantization with $\mu_0$=8 and $\varepsilon_0$= 8.5. (c) The displayed wavelet coefficients (d) Edge image of displayed coefficients

### 4.2.3 Channel coding and noise

A MATLAB™ function was developed to simulate channel noise and image transmission using JPEG2000 standards. This function was then used to simulate image transmission and image corruption due to channel noise. The added noise to the channel is

the burst noise, the two-state Markov channel model was used to simulate the burst noise transmission channel. This two-state Markov channel model consists of state *G* and state *B*. In state *G*, it is assumed to achieve error-free transmission. In state *B*, the probability of transmitting any specific digit correctly is *h*. So, the probability of making an error in the state *B* (the *Bad* state) is $P_{Eb}$ which was assumed to be 1. The transition from *Bad* state to *Good* state has a probability $P_{bg}$ and it was assumed to be 0.25. *BER* (Bit Error Rate) is then determined by simply making a change in the transition probability from *Good* state to *Bad* state, $P_{gb}$. The following equation was used to calculate the BER [44]:

$$BER = P_{Eb}\frac{P_{gb}}{P_{gb}+P_{bg}} \quad (20)$$

After generating the two-state Markov noise, this noise was added logically to the binary Huffman coding data. The method of addition was done simply by applying the EXCEXLUSIVE OR logical operation and the result was an image with noise distortion. Thus image mixed with noise is transmitted using JPEG2000 protocols and is the one received at the receiver. The image that contains the edges is a binary image. This binary image of the edges can be compressed and channel coded using any power and robust (i.e., error free) protocols for binary image. The binary image being very small in size compared to compressed image, does not affect significantly the compression ratio.

**Experimental Justification:**

Back to Figure 4.9, the size of the wavelet coefficients for the JPEG2000 approximation is 63 KB. Any forward error concealment technique will require adding a controlled amount of redundancy which may extend the size of the wavelet coefficients to go beyond 150 KB. Whereas, the size of the edge image is 3 KB only, and channel coding of the edge image will add up to 9 KB extra size to the wavelet coefficients. Thus the proposed approach can be considered efficient in reducing bandwidth requirements, and can be exploited further at the receiver for additional advantages. This is illustrated in the next chapter.

### 4.2.4 The receiver

Once the image is received, the edge extraction is first computed for received coefficients as discussed in section 4.1.2. The new edge extraction is then subtracted from the received one to determine the corrupted regions resulting from the image transmission. The Figure 4.10(a) shows the received image reconstructed after passing through noisy transmission channel

with *BER* = 0.009. The Figure 4.10(b) shows the displayed wavelet coefficients of the received image, the Figure 4.10(c) shows the edge extraction of displayed wavelet coefficients, and the Figure 4.10(d) shows the location of the corrupted regions resulting by subtracting the extracted edge information of received coefficients from the received edge data of coefficients of the original image.

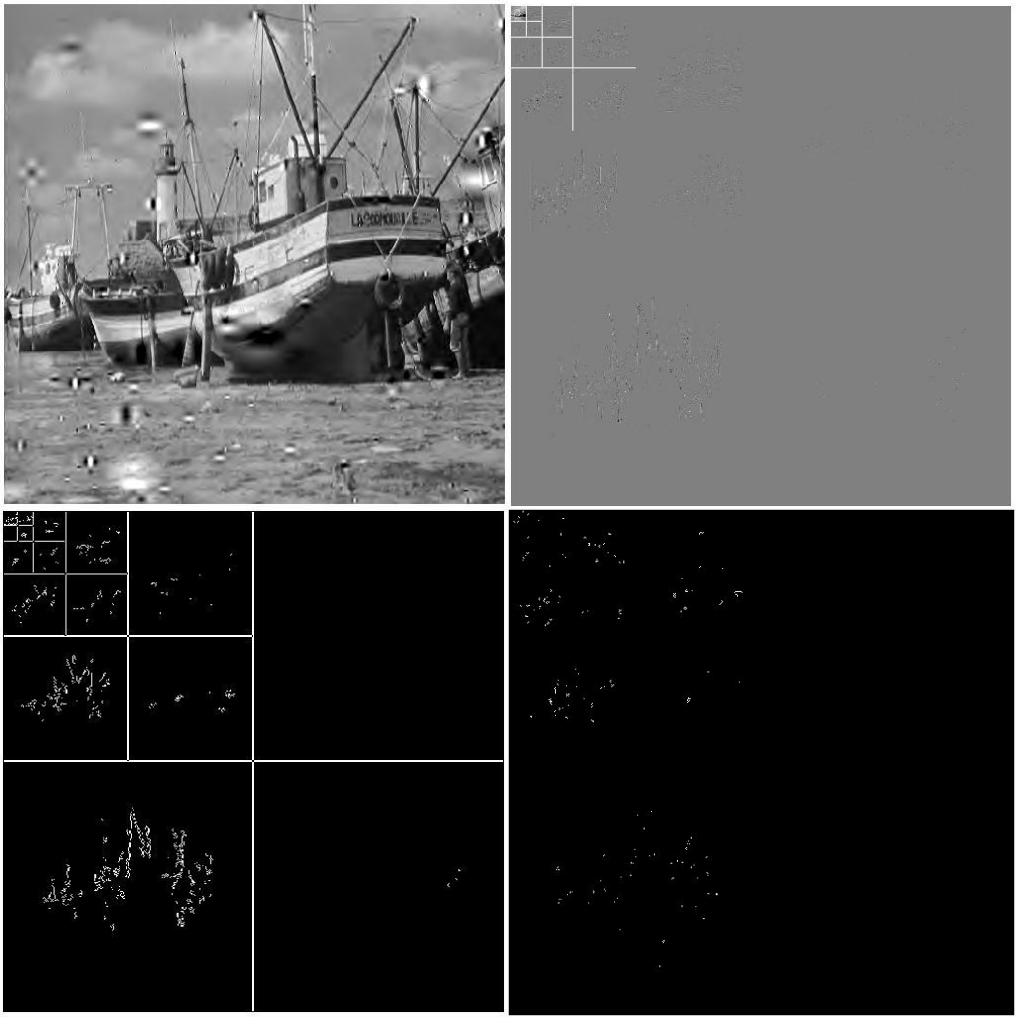

**Figure 4.10:** (a) Top left: Original image received with BER=0.009 (b) Top right: The displayed wavelet coefficients (c) Bottom left: Edge extraction of received wavelet coefficients (d) Bottom right: Result of subtracting extracted edge image from the received edge image

# Chapter 5

# Results and Discussions

The five 512 × 512 8-bit monochrome famous images were chosen to test the proposed approach. The Figure 5.1 shows five images: *woman, pirate, boat, goldhill* and *baboon* respectively. The first two images are with a low level of detail, the second two images are with a medium level of detail and the last image is with a relatively large amount of detail.

**Figure 5.1:** Test images (a) *woman* (b) *pirate* (c) *boat* (d) *goldhill and* (e) *baboon*

All images were compressed using a five-scale wavelet transform with an implicit quantization, $\mu_0$=8 and $\varepsilon_0$= 8.5. After that, channel coding was applied to all images with bit error rate (BER) equal to 0.004, 0.006 and 0.009 to represent different noise scenarios (low, medium and high). The suggested methodology was applied for image concealment and results were analyzed using visual comparison, comparing values of root mean square error (rms) as well as values of peak signal-to-noise ratio (PSNR). In the following, part1 results discuss *boat* image with BER 0.009 and using different types of error concealing methods. Based on this, the method with best results is discussed in part 2, where this approach is applied to all other images with different BER values.

## 5.1 Part 1 Results

The Figure 5.2 shows the compressed image with its wavelet coefficients. This image is sent through a communication channel where it is mixed with a two-state Markov channel model having BER = 0.009. This results in the received image shown in Figure 5.3. The Figure 5.3(left) shows the noisy received image with big blurs resulting from the noise hitting lower sub-bands and small blurs resulting from the noise to higher sub-bands. The right part of the Figure shows wavelet coefficients of the received image. The Figure 5.4(left) shows edges of the sent image. As discussed in chapter 4, this edge information is assumed to be received uncorrupted, while Figure 5.4(center) shows edge extraction of the received image using Canny method and Figure 5.4(right) is the difference between left and right edge images. This difference is calculated to identify locations of corrupted coefficients.

**Figure 5.2:** (Left) Sent image; (Right) Its wavelet coefficients

**Figure 5.3:** (Left) Received corrupted image; (Right) Its wavelet coefficients

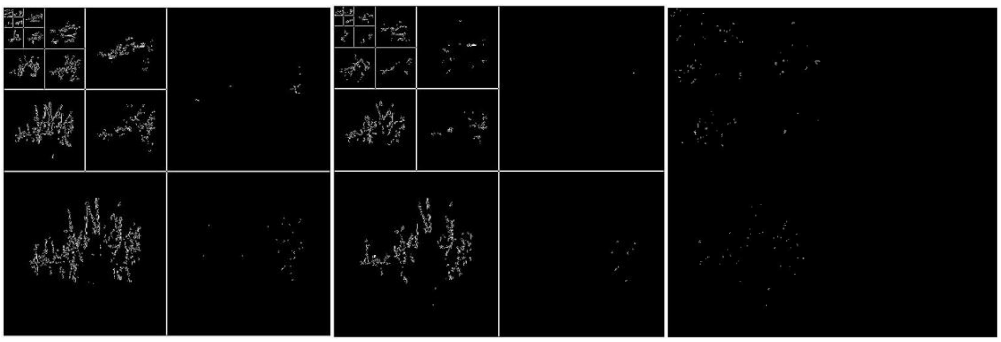

**Figure 5.4:** (left) Edge image of wavelet coefficients of the sent image; (center) Extracted edge image of wavelet coefficients of received image; (right) The difference between left and center images

After difference between edge images is calculated and locations of corrupted coefficients are identified, three methods were applied to do error concealment:

Method 1: For approximation coefficients sub-band level ($a_5HH$ sub-band), the value of each corrupted coefficient is estimated by taking the average value of eight surrounded coefficients. Then all corrupted coefficients on remaining sub-bands are simply set to zero.

Method 2: For approximation coefficients sub-band level ($a_5HH$ sub-band), the value of each corrupted coefficient is estimated by using the median filter (taking the median value of the nine coefficients in 3x3 neighborhood). Then all corrupted coefficients on remaining sub-bands are simply set to zero.

Method 3: It expands method 2 to other sub-bands on the lowest level (level 5). This means that all corrupted coefficients for all sub-bands on level 5 are estimated using median filter on 3x3 neighborhood of the corrupted coefficient. The rest of corrupted coefficients on the higher sub-bands are simply set to zero.

**Figure 5.5:** (Left) The concealed image using method-1 (Center) The concealed image using method-2 (Right) The concealed image using method-3

| Boat with BER=0.009 | RMS | PSNR (dB) |
|---|---|---|
| Received Image | 17.36 | 23.34 |
| Concealed Method-1 | 3.22 | 37.99 |
| Concealed Method-2 | 2.76 | 39.33 |
| Concealed Method-3 | 2.70 | 39.50 |

**Table 5.1:** The rms and PSNR values for three concealment methods with channel BER=0.009

The Figure 5.5 shows results of three methods, while Table 5.1 shows rms and PSNR values for the received corrupted image and after it has been processed using three error concealment methods just described above. From Figure 5.5, it can be noticed that blurs are successfully concealed in all three processed images with few noticeable differences. The image in Figure 5.5 (a) has new light blur under the boat. This blur has resulted due to estimation done using the mean filter on $a_5HH$ sub-band. Comparing it with the image on Figure 5.5(b), it is obvious that the median filter has successfully concealed corrupted coefficients with no new resulting blur. However, simple eye observation cannot define real difference between Figure 5.5(b) and Figure 5.5(c).

The Table 5.1 shows that the rms value 17.36 of the corrupted received image has been reduced to 3.22 using method-1, 2.76 in method-2 and 2.70 in method-3. The same statement can be made regarding PSNR values. The PSNR 23.34 dB of the received image has improved to 37.99 dB using method-1, 39.33 using method-2, and 39.5 using method-3.

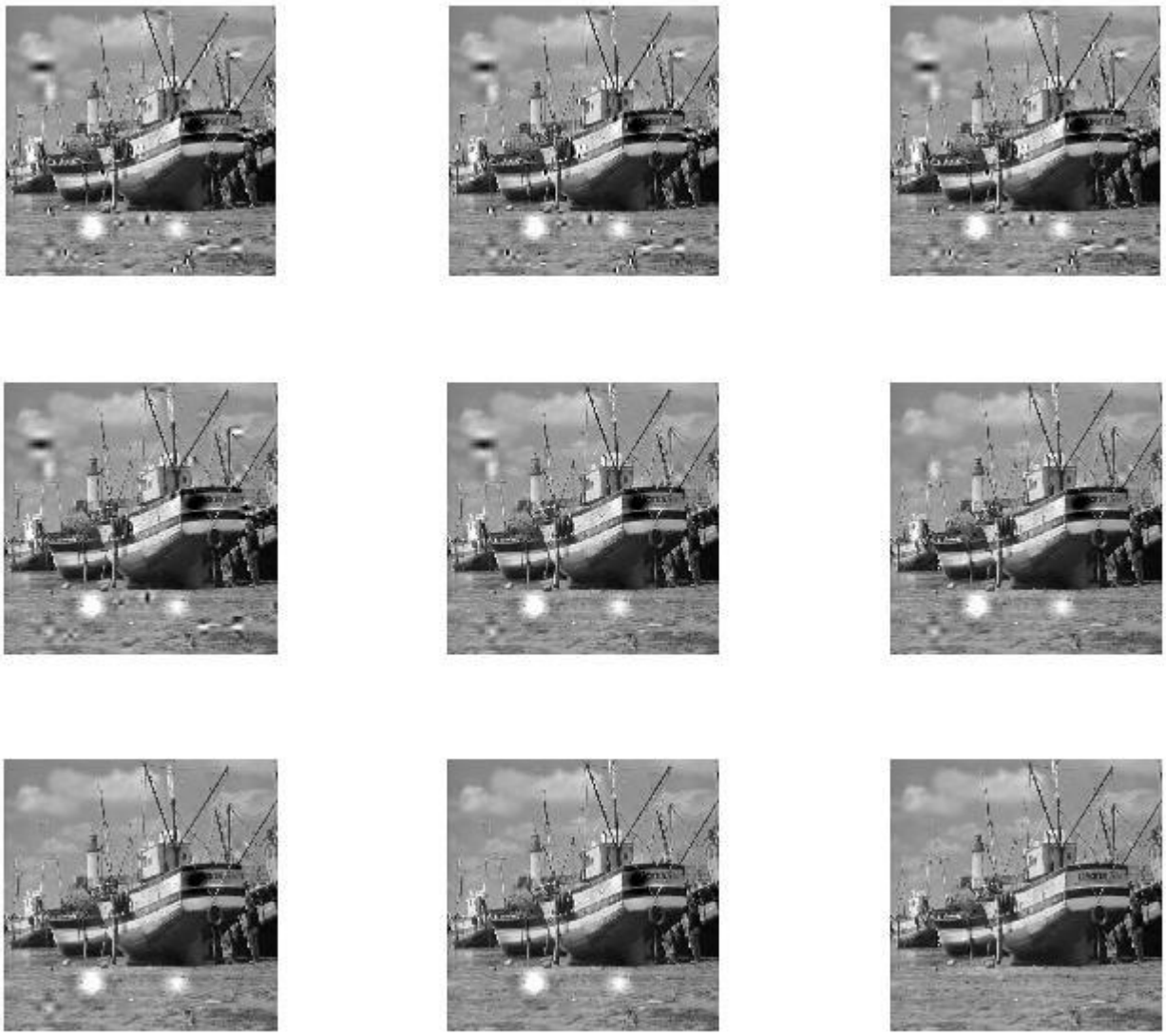

| | | |
|---|---|---|
| a | b | c |
| d | e | f |
| g | h | i |

**Figure 5.6:** The concealment steps in method-3 with BER=0.009: (a) received image (b)-(e) respectively, shows the image after concealment on each level starting from level 1 to level 4 (f) shows image after concealment on $a_5HL$ sub-band (g) shows image after concealment on $a_5LL$ sub-band (h) shows image after concealment on $a_5HH$ sub-band (i) shows image after concealment on the $a_5LL$ sub-band

Comparing the results of Table 5.1, it is obvious that method-2 and method-3 are much better from method-1. Additionally, method-3 performs slightly better than method-2 based on the results of rms and PSNR. Therefore, it seems better and safer to use method-3 because coefficients on all lower sub-bands are important and could always have a blurring effect on a wide range of pixels in the spatial domain. In Figure 5.6, step by step concealment of

method-3 is shown: (a) is the received image, (b)-(e) respectively shows the image after concealment on each level starting from level 1 to level 4, (f) shows the image after concealment on $a_5HL$ sub-band, (g) shows the image after concealment on the $a_5LL$ sub-band, and (h) shows the image after concealment on $a_5HH$ sub-band. Finally (i) shows image after concealment on $a_5LL$ sub-band (the fully concealed image).

a b
c d
e f

**Figure 5.7:** The received and concealed images for woman image: (a) and (b) for BER=0.004; (c) and (d) for BER = 0.006; (e) and (f) for BER=0.009

### 5.1.1 Computational Complexity

The three methods used in previous section involve edge extraction for the received coefficients, binary subtraction of edge data, and the selective filter operation on coefficients. The computational complexity of subtraction can be ignored because it can be done easily in

real time as it is a simple logical operation. The computational complexity for the mean and the median operations is of the order of $O(n)$ and $O(n \log n)$ respectively [45-46], while the computational complexity for edge extraction using Canny edge detector operation is $O(dim^2)$, where *dim* is the dimension of the bounding rectangle containing the object [47]. Thus, the computation complexity for both method 1 and method 2 can be written as:

$$C_1 = C_{mean} + C_{edge\ extraction} = M_1 * O(n) + O(dim^2) \quad (21)$$

$$C_2 = C_{median} + C_{edge\ extraction} = M_1 * O(n \log n) + O(dim^2) \quad (22)$$

where $M_1$ stands for the number of corrupted coefficients at the approximation sub-band. Similarly, the computational complexity for method 3 can be written as:

$$C_3 = M_1 * O(n \log n) + M_2 * O(n \log n) + M_3 * O(n \log n) + M_4 * O(n \log n) + O(dim^2)$$

$$C_3 = [M_1 + M_2 + M_3 + M_4]\ O(n \log n) + O(dim^2) \quad (23)$$

where $M_1$ is the number of corrupted coefficients at the approximation sub-band, and $M_2 - M_4$ are the number of corrupted coefficients at the low sub-bands of level 5.

### 5.2 Part 2 Results

In Part 2, the method-3 was applied for all pictures shown in Figure 5.1. Each image was transmitted through the system with three different BER values (0.004, 0.006 and 0.009). The results of received and concealed images are shown on the following Figures (from Figure 5.7 to Figure 5.11 each for the images *woman*, *pirate*, *boat*, *goldhill* and *baboon* respectively). It is possible to observe by visual comparison that all the blurs resulting by the channel noise have mostly been removed using method-3 and a good level of perpetual quality generally restored even with the image of a relatively large amount of details (i.e., baboon).

The Table 5.2 shows values of rms and PSNR for all five test images using error concealment method-3 with three BER values (0.004, 0.006 and 0.009). It is obvious from the Table that rms values get higher as BER is increased. However, after concealment using method-3, the rms values are dramatically decreased. As an example of woman image with BER=0.006, the rms value is decreased from 6.37 to 0.98 and for the same BER, the rms value of Goldenhill image is decreased from 9.4 on the received image to 1.93 on the concealed image. In general, rms values reached very acceptable ranges after concealment. Most of the rms values are below 3 while in some cases it is higher than 3 (e. g. Pirate with BER = 0.006) but the concealed image is still very acceptable using visual comparison.

Likewise, the PSNR values after concealment always improved to values above 35 dB, which is better than the results claimed in [28]. The range of improvement is between 10 dB and 12 dB (even for BER=0.009), which is better than ranges of 2 dB reported in [26] and range of 6.5 db reported in [29].

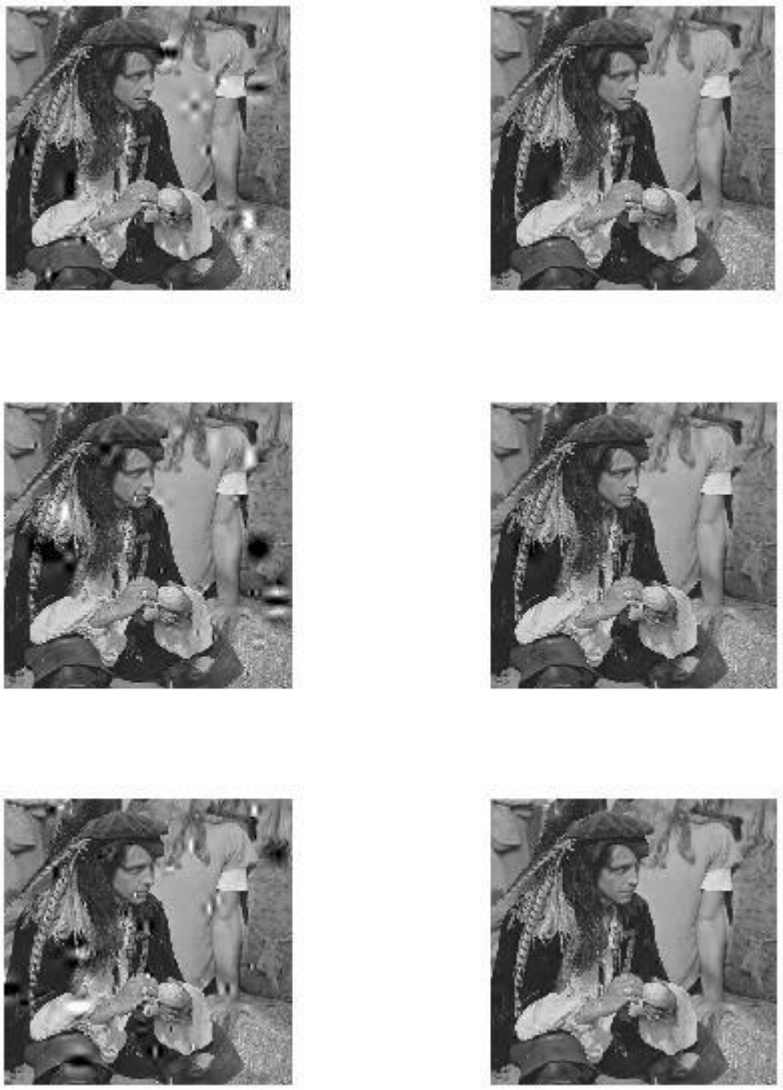

a B
c D
e F

**Figure 5.8:** The received and concealed images for Pirate image: (a) and (b) for BER=0.004; (c) and (d) for BER=0.006; (e) and (f) for BER=0.009

a b
c d
e f

**Figure 5.9:** The received and concealed images for boat image: (a) and (b) for BER=0.004; (c) and (d) for BER=0.006; (e) and (f) for BER=0.009

a B
c D
e F

**Figure 5.10:** The received and concealed images for Goldhill image: (a) and (b) for BER=0.004; (c) and (d) for BER=0.006; (e) and (f) for BER=0.009

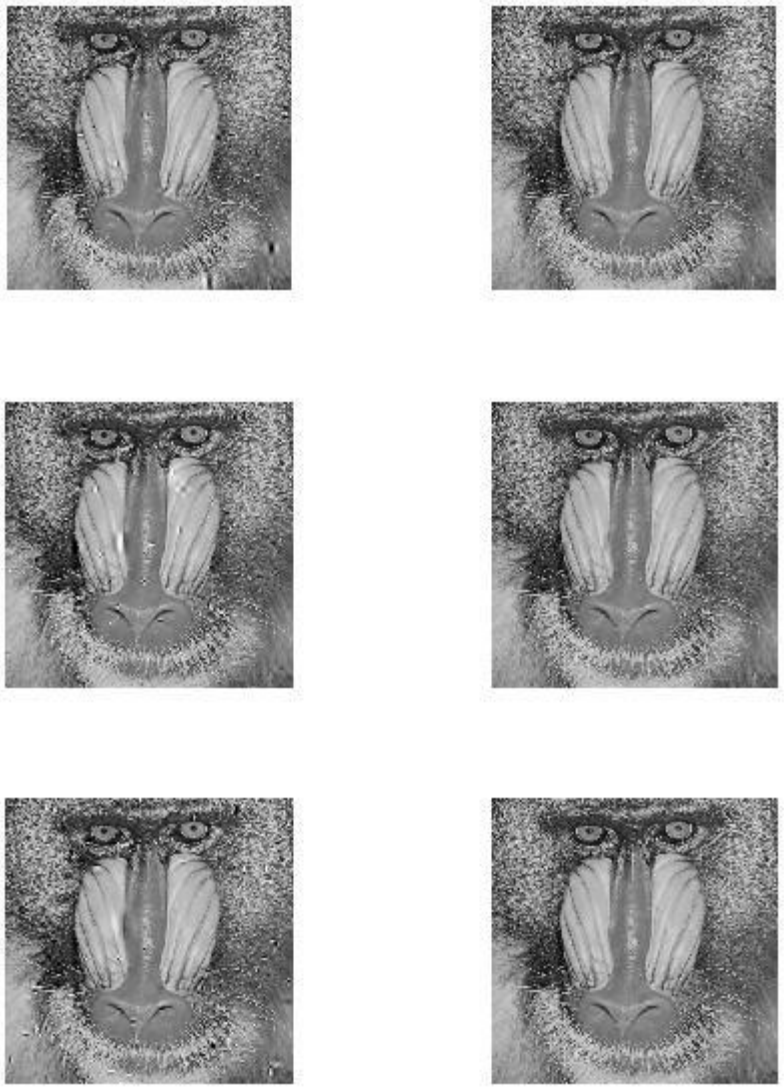

a B
c d
e f

**Figure 5.11:** The received and concealed images for Baboon image: (a) and (b) for BER=0.004; (c) and (d) for BER=0.006; (e) and (f) for BER=0.009

| Woman image | Received Image | | Concealed Image | |
|---|---|---|---|---|
| | RMS | PSNR (dB) | RMS | PSNR (dB) |
| BER=0.004 | 5.28 | 33.68 | 1.17 | 46.74 |
| BER=0.006 | 6.37 | 32.04 | 0.98 | 48.28 |
| BER=0.009 | 9.78 | 28.33 | 2.91 | 38.84 |
| Pirate image | Received Image | | Concealed Image | |
| | RMS | PSNR (dB) | RMS | PSNR (dB) |
| BER=0.004 | 11.68 | 26.78 | 1.69 | 43.55 |
| BER=0.006 | 13.53 | 25.50 | 3.92 | 36.27 |
| BER=0.009 | 12.86 | 25.94 | 2.20 | 41.29 |
| Boat image | Received Image | | Concealed Image | |
| | RMS | PSNR (dB) | RMS | PSNR (dB) |
| BER=0.004 | 8.54 | 29.50 | 2.09 | 41.72 |
| BER=0.006 | 12.22 | 26.39 | 3.60 | 37.02 |
| BER=0.009 | 17.36 | 23.34 | 2.70 | 39.50 |
| Goldhill image | Received Image | | Concealed Image | |
| | RMS | PSNR (dB) | RMS | PSNR (dB) |
| BER=0.004 | 9.28 | 28.78 | 3.99 | 36.10 |
| BER=0.006 | 9.40 | 28.67 | 1.93 | 42.34 |
| BER=0.009 | 10.71 | 27.54 | 2.39 | 40.45 |
| Baboon image | Received Image | | Concealed Image | |
| | RMS | PSNR (dB) | RMS | PSNR (dB) |
| BER=0.004 | 7.50 | 30.63 | 2.42 | 40.47 |
| BER=0.006 | 8.59 | 29.45 | 3.02 | 38.52 |
| BER=0.009 | 10.56 | 27.66 | 3.55 | 37.12 |

**Table 5.2:** The rms and PSNR values for the concealed method 3 used on test images with channel BER=0.004, 0.006, 0.009

# Chapter 6

# Conclusions and Suggested Future Work

In this chapter, the final conclusions reached at the end of the thesis are drawn. Furthermore, possible directions for future research are also suggested.

## 6.1 Conclusions

The main functions of this work included developing a method to determine corrupted coefficients in wavelet domain, concealing errors by setting the values of the corrupted coefficients to zero or estimating these coefficients using its adjacent neighbors, and compatibility with JPEG2000 standard. The corrupted coefficients were determined by subtracting received edge image from extracted edge image. Three methods were developed for error concealment. The first method applied mean filter to the corrupted coefficients' neighborhood in the approximation sub-band, and set determined corrupted coefficients in other sub-bands to zero. The second method applied median filter to the corrupted coefficients' neighborhood on the approximation sub-band and set determined corrupted coefficients in other sub-bands to zero. The third method is the same as the second but median filter is also extended to the corrupted coefficients on the lower sub-bands.

The five 512 × 512 8-bit monochrome images were chosen to test the proposed approach. The images were chosen with a diversity in detail: two images with low level of detail, two images with medium level of detail and one with a relatively large amount of detail. Three bit error rates were used to represent different noise scenarios. By analysis of the results, it was shown that method-2 and method-3 were much better than method-1. Additionally, method-3 performed slightly better than method-2 based on the results of rms and PSNR. Overall, improvements in rms and PSNR values were significant and can be easily compared to claimed improvements reported in the literature.

The combination of compressed image transmission based on JPEG2000 standard, and error concealment using either method-2 or method-3 ensures minimized requirement for channel bandwidth. Furthermore, all steps of the approach are done in wavelet domain and that the proposed approach does not involve any iteration in the loop. Rather, the steps of the approach involve only edge extraction, subtraction between two binary images, and filtering on selected sub-bands before image is decompressed and decoded using JPEG2000. Because

of the nature of wavelet domain, filtering of selected sub-bands can be implemented in parallel, thus making this approach less expensive on computations.

## 6.2 Suggestions for Future Work

The work in this thesis can be extended to different directions. Some of the ideas are listed below.

### 6.2.1 Developing a mathematical algorithm to determine exact values of corrupted coefficients

Although the JPEG2000 compression is mathematically lossy, it could be possible to develop a mathematical method that can estimate a very similar value to the corrupted coefficients if these coefficients are in the lower sub-band level or on the approximation level. Mathematical relationship may be explored between any corrupted coefficient in the lower sub-band and its corresponding coefficients at the higher sub-band and from the approximation coefficients. For approximation level, mathematical relationship might be also found between the corrupted coefficients and its uncorrupted adjacent coefficients or its corresponding coefficients on the lower sub-band level. Once mathematical relationships are found, error concealment would be easier to accomplish.

### 6.2.2 Parallel Processing Implementation

This is going to improve the speed of the concealment method. As seen on Fig. 5.6, the error concealment was done level by level. Error concealment on each level is purely independent according to the proposed concealment method. This can allow parallel processing to be implemented to increase the speed of the operation.

# References


[1] http://www.jpeg.org, accessed on November 5, 2011

[2] Gonzalez, Rafael C. and Richard E. Woods, Digital Image Processing, Upper Saddle River, NJ: Prentice-Hall, 2008.

[3] P. Schelkens, A. Skodras & T. Ebrahimi. The JPEG 2000 Suite. Wiley, Series: Wiley-IS&T Series in Imaging Science and Technology, 2009

[4] Qurban Memon and Takis Kasparis, "Signal Decomposition and Coding using a multiresolution transform", *International Journal of Systems Sciences*, Vol. 29 No. 2, pp. 111-120, Feb. 1998.

[5] Qurban Memon and Takis Kasparis, "Transform Coding of signals using Approximate Trigonometric Expansions", *Journal of Electronic Imaging*, Vol. 6, No. 4, pp. 494-503, October, 1997.

[6] Qurban Memon, "Synchronized Chaos for Network Security", *Computer Communications*, Vol. 26, No. 6, pp. 498-505, April 2003.

[7] Qurban Memon, "WPT based Fast Multiresolution Transform", *Malaysian Journal of Computer Science*, Vol. 15, No. 1, pp. 28-36, 2002.

[8] Qurban Memon, "Online Security Techniques for Processing of Video", *Proceedings of IEEE International Conference on Telecommunications*, Volume 1, pp. 840-844, June 23-26, 2002, Beijing, China.

[9] Qurban Memon and Zahid Ali, "Network Security in Video Communications using Choatic Systems", *Proceedings of International VCIP 2000 Conference,* Perth, Australia, Vol. No. 4067-33, pp. 1164-1174, June 2000.

[10] http://fourier.eng.hmc.edu/e161/lectures/wavelets/node8.html, accessed on November 7, 2011

[11] http://www.aai.ee/data/midas/volb/node316.html, accessed on November 7, 2011

[12] S. Mallat, "A Theory for Multiresolution Signal Decomposition: The Wavelet Representation," *IEEE Transactions on Pattern Analysis and Machine Intelligence*, Vol. 11, pp. 674-693, July 1989.

[13] A. Cohen, I. Daubechies, and J.-C. Feauveau, "Biorthogonal bases of compactly supported wavelets," *Communications on Pure Applied Mathematics*, 45(5), 1992.

[14] Qurban Memon, "Interference Rejection and Noise Removal from DS-Spectrum Receivers using Multiresolution Transform", *Electronic Journal of School of Advanced technologies,* Volume 3, Issue 1, April 2001.

[15] Takis Kasparis, Michael Georgiopoulos and Qurban Memon, "Direct-Sequence Spread-Spectrum with Transform domain Interference Suppression", *International Journal of Circuits, Systems, and Computers,* Vol.5, No.2, pp.167-179, 1995.

[16] Qurban Memon, "Signal Transmission through CDMA Channels employing Multiresolution Transmission", *Proceedings of ICSPAT 2000*, Paper No. 60, pp. 300-304, Dallas, Texas, USA.

[17] Qurban Memon, "Interference Rejection in Wireless Communications using Approximation in Transform Domain", *International Wireless and Telecommunications Symposium*, Kuala Lumpur, Malaysia, pp. 411-414, May 13-15, 1998.

[18] S. Khalid, *Introduction to Data Compression*, New York, Morgan Kaufmann Publishers, 2000

[19] L. Hanzo, P. Cherriman, J. Streit, *Wireless Video Communications: IEEE Series*, NY: IEEE Press, 2001.

[20] Y. Wang and Q. Zhu, "Error control and concealment for video communication: A Review," *Proceedings of the IEEE,* Vol. 86, No. 5, pp. 974-996, May 1998.

[21] V. Goyal, J. Kovacevic, "Generalized Multiple Description Coding with Correlating Transforms," *IEEE Transactions on Information Theory,* Vol. 47, pp. 2199-2224, Sep. 2001

[22] S. Hemami, "Robust Image Transmission using Re-synchronizing Variable-length Codes and Error Concealment", *IEEE Journal on Selected Areas in Communications*, June 2000

[23] I. Moccagatta, S. Soudagar, j. Liang, H. Chen, "Error-Resilient Coding in JPEG-2000 and MPEG-4" *IEEE Journal on Selected Areas in Communications*, June 2000

[24] S. W. Lin, J. J. Leou, and L. W. Kang, "An error resilient coding scheme for H.26L video transmission based on data embedding," *Journal of Visual Communications and Image Representation,* vol. 15, no. 2, pp. 214-240, June 2004

[25] A. Kaup, K. Meisinger ,Til Aach, "Frequency Selective Signal Extrapolation with Applications to Error Concealment in Image Communication," *International Journal of Electronic Communications (AE-),* No. 59, pp. 147-156, Elsevier GmbH, 2005

[26] K. Meisinger, J. Garbas, A. Kaup, "Error control and concealment of JPEG2000 coded image data in error prone environments." *Proceedings of the picture coding symposium* (PCS). San Francisco, December 2004

[27] L. Ramac and P. K. Varshney, “A Wavelet domain diversity method for transmission of images over wireless channels,” *IEEE Journal on Selected Areas in Communications,* Vol. 18, No. 6, pp. 891-898, June 2000

[28] M. Bingabr and P.K. Varshney, “Recovery of Corrupted DCT Coded Images Based on Reference Information” *IEEE Transactions on Circuit and Video Systems*, Vol. 14, No.4, pp. 441-449, April 2004.

[29] L. Atzori, Giaime Ginesu and Alessio Raccis “JPEG2000-Coded Image Error Concealment Exploiting Convex Sets Projections” *IEEE Transactions on Image Processing*, Vol. 14, No. 4, April 2005

[30] L. Atzori, D. Giusto, and A. Raccis, “High frequency error concealment in wavelet-based image coding,” *Electronic Letters*, Vol. 39, No. 2, pp. 203–205, Jan. 2003

[31] A. Kaupa, K. Meisingera, T. Aachb “Frequency selective signal extrapolation with applications to error concealment in image communication” *International Journal of Electronic Communications*, pp:147-156, March 2005

[32] Lowe, David and Bennett, Michael J., "A Status Report on JPEG 2000 Implementation for Still Images: The UConn Survey" (2009), *UConn Libraries Presentations*, Paper 21

[33] A. J. Pinho, L. B. Almeid. "A review on edge detection based on filtering and differentiation," *REVISTA DO DETUA*, Vol. 2, No 1, pp. 113-126, September 1997.

[34] J. Canny, “A Computational Approach to Edge Detection,” IEEE Transactions on Pattern Analysis, Vol. PAMI-8, No. 6, pp. 679-698, Nov. 1986.

[35] Y.J. Jung, M. Hahn, Y.M. Ro, "Spatial Frequency Band Division in Human Visual System Based-Watermarking", *Proceedings of IWDW*, 2002, pp.224-234.

[36] Shu Lin, Daniel J. Costello, Jr., *Error Control Coding: Fundamentals and Applications*, Prentice Hall, 1983, ISBN 0-13-283796-X

[37] Qurban Memon, Takis Kasparis, “Block Median Filters”, *SPIE’s International AeroSense Symposium*, Orlando, 1995, vol. 2488, pp. 100-109.

[38] Takis Kasparis, Qurban Memon, Revathi Koteeswaran, “Rank Filters with Adaptive Length”, *SPIE’s International AeroSense Symposium*, Orlando, 1994, vol. 2239, pp. 256-266.

[39] J. R. Taylor, An Introduction to Error Analysis: The Study of Uncertainties in Physical Measurements, University Science Books, p. 94, §4.1, 1999, ISBN 093570275X

[40] Federal Standard 1037C, http://www.its.bldrdoc.gov/fs-1037/, accessed on November 4, 2011

[41] Douglas R. Stinson, CRYPTOGRAPHY Theory and Practice, Second Edition, Chapman & Hall/CRC, 2002.

[42] http://www.wireshark.org/docs/wsug_html_chunked/ChAdvChecksums.html, accessed on November 15, 2011

[43] Stephen B. Wicker, Error Control Systems for Digital Communication and Storage, Prentice Hall, 1995

[44] E. N. Gilbert, "Capacity of a burst-noise channel," *Bell Syst. Technical Journal*, pp. 1253–1266, Sept. 1960.

[45] http://www.cs.cmu.edu/~mblum/research/pdf/grad.html, accessed on January 24, 2011

[46] C. P. Schnorr and G. Stumpf. A characterization of complexity sequences. Zeitschrift fur Mathematische Logik und Grundlagen der Mathematik 21(1):47–56, 1975.

[47] Kuhn Beoldri, L. Beolchi, M. H. Kuhn, Medical Imaging, Analysis of Multimodality 2D/3D Images, IOS Press, P:114, 1995

# الإرسال القوي للصور بنظام جي بيج ٢٠٠٠ باستخدام معلومــات الحافــة

أمجد نزيه بومطر

يناير ٢٠١٢

## ملخص الرسالة

إن عملية ضغط البيانات عملية جوهرية وأساسية في مجال اتصالات الوسائط المتعددة وتخزين البيانات، حيث أنها تعمل على زيادة سرعة نقل البيانات، وتقليل عرض النطاق الترددي لقناة الاتصال، بالإضافة إلى خفض السعة المطلوبة لتخزين . الجي بيج ٢٠٠٠ هو المعيار الجديد لضغط الصور بغرض الإرسال والتخزين، من عيوب عملية ضغط البيانات تلك هو أن البيانات المضغوطة تصبح أكثر عرضة للتشويش أثناء عملية الإرسال.

التقنيات السابقة لعمليات إخفاء الخطأ تصنف إلى ثلاثة مجموعات تبعاً للمنهجة المستخدمة في عملية التشفير وفك التشفير وهي: إخفاء الخطأ المبكر، إخفاء الخطأ بعد المعالجة، وإخفاء الخطأ التفاعلي. الهدف من هذه الأطروحة هو وضع منهجية إخفاء لديها القدرة على اكتشاف الخطأ وإخفائه معاً، وتكون في نفس الوقت متوافقة مع معيار الجي بيج ٢٠٠٠، وتضمن أيضاً استخدام الحد الأدنى من عرض النطاق الترددي لقناة الاتصال.

تم تطوير منهجية جديدة للكشف عن المناطق \ المعاملات التالفة في الصورة المستلمة باستخدام معلومات الحافة، هذه المنهجية تتطلب إرسال معلومات الحافة لمعاملات مويّجات الصورة الأصلية مع الصورة المضغوطة بتقنية جي بيج ٢٠٠٠، وعند استقبال المعلومات المرسلة، يتم حساب معلومات الحافة لمعاملات المويّجات المستقبلة ومن ثم مقارنتها بمعلومات الحافة لمعاملات مويّجات الصورة الأصلية لتحديد المعاملات التالفة، تم التحقق من ثلاثة طرق للإخفاء باستخدام المرشح لمعالجة المناطق \ المعاملات التالفة.

تم تطوير برمجيات باستخدام برنامج الماتلاب لمحاكاة عملية التشويش، وإرسال الصورة باستخدام معيار الجي بيج ٢٠٠٠ وفقا للمنهجية المقترحة، استخدمت طرق قياس الجودة مثل: نسبة ذروة الإشارة إلى التشويش، جذر المتوسط التربيعي للخطأ، و قياس الجودة الذاتي؛ وذلك لتقييم الصور المعالجة، عرضت نتائج المحاكاة لشرح أداء المنهجية المقترحة، تم أيضا مقارنة النتائج مع أحدث المنهجيات في النشرات العلمية، وبناء على أداء المنهجية المقترحة، يمكن اعتبارها قابلة للاستخدام بنجاح في مجال الاتصالات اللاسلكية والإنترنت.

UAEU Faculty of Engineering

جامعة الإمارات العربية المتحدة
United Arab Emirates University

# الإرسال القوي للصور بنظام جي بيج ٢٠٠٠ باستخدام معلومـات الحافـة.


عمل:
أمجد نزيه بومطر

مشرف الرسالة:
د. قربان علي مأمون


هذه الرسالة قُدمت إلى كلية الهندسة - قسم الهندسة الكهربائية بجامعة الإمارات العربية المتحدة كجزء من متطلبات الحصول على درجة الماجستير في الهندسة الكهربائية

UAEU Faculty of Engineering

جامعة الإمارات العربية المتحدة
United Arab Emirates University

# الإرسال القوي للصور بنظام جي بيج ٢٠٠٠ باستخدام معلومـات الحافـة.


عمل:
أمجد نزيه بومطر

مشرف الرسالة:
د. قربان علي مأمون


يناير ٢٠١٢